Blood proteomics and multimodal risk profiling of human volunteers after incision injury: A translational study for advancing personalized pain management after surgery

Daniel Segelcke [a,1], Julia R. Sondermann [b,1], Christin Kappert [c], Bruno Pradier [d], Dennis Görlich [e], Manfred Fobker [f], Jan Vollert [a,g], Peter K. Zahn [h], Manuela Schmidt [b,*,2], Esther M. Pogatzki-Zahn [a,**,2]

[a] Department of Anaesthesiology, Intensive Care and Pain Medicine, University Hospital Muenster, Albert-Schweitzer-Campus 1, Muenster 44651, Germany
[b] Department of Pharmaceutical Sciences, Division of Pharmacology and Toxicology, Systems Biology of Pain Group, University of Vienna, UZA II, Josef-Holaubek-Platz 2, Vienna A-1090, Austria
[c] Max-Planck Institute for Multidisciplinary Sciences, City Campus, Hermann-Rein-Straße 3, Göttingen 37075, Germany
[d] Department of Anaesthesiology, Intensive Care and Pain Medicine, University Hospital Muenster, Muenster, Germany
[e] Institute of Biostatistics and Clinical Research, University of Münster, Albert-Schweitzer-Campus 1, Münster 44651, Germany
[f] Centre of Laboratory Medicine, University Hospital Muenster, Albert-Schweitzer-Campus 1, Muenster 44651, Germany
[g] Department of Clinical and Biomedical Sciences, Faculty of Health and Life Sciences, University of Exeter, Exeter, UK
[h] Department of Anesthesiology, Intensive Care and Pain Medicine, BG University Hospital Bergmannsheil, Ruhr-Universität Bochum, Bürkle de la Camp-Platz 1, Bochum 44789, Germany

ARTICLE INFO

ABSTRACT

A significant number of patients develop chronic pain after surgery, but prediction of those who are at risk is currently not possible. Thus, prognostic prediction models that include bio-psycho-social and physiological factors in line with the complex nature of chronic pain would be urgently required. Here, we performed a translational study in male volunteers before and after an experimental incision injury. We determined multi-modal features ranging from pain characteristics and psychological questionnaires to blood plasma proteomics. Outcome measures included pain intensity ratings and the extent of the area of hyperalgesia to mechanical stimuli surrounding the incision, as a proxy of central sensitization. A multi-step logistic regression analysis was performed to predict outcome measures based on feature combinations using data-driven cross-validation and prognostic model development. Phenotype-based stratification resulted in the identification of low and high responders for both outcome measures. Regression analysis revealed prognostic proteomic, specific psychophysical, and psychological features. A combinatorial set of distinct features enabled us to predict outcome measures with increased accuracy compared to using single features. Remarkably, in high responders, protein network analysis suggested a protein signature characteristic of low-grade inflammation. Alongside, *in silico* drug repurposing highlighted potential treatment options employing antidiabetic and anti-inflammatory drugs. Taken together, we present here an integrated pipeline that harnesses bio-psycho-physiological data for prognostic prediction in a translational approach. This pipeline opens new avenues for clinical application with the goal of stratifying patients and identifying potential new targets, as well as mechanistic correlates, for postsurgical pain.

* Corresponding author at: Department of Pharmaceutical Sciences, Division of Pharmacology and Toxicology, Systems Biology of Pain Group, University of Vienna, UZA II, Josef-Holaubek-Platz 2, Vienna A-1090, Austria.
** Correspondence to: Department of Anaesthesiology, Intensive Care and Pain Medicine, University Hospital Muenster, Albert-Schweitzer-Campus 1, A1, Muenster 48149, Germany.
E-mail addresses: manuela_schmidt@univie.ac.at (M. Schmidt), pogatzki@anit.uni-muenster.de (E.M. Pogatzki-Zahn).
[1] These authors contributed equally to this work.
[2] These senior authors contributed equally to this work.

1. Introduction

It is estimated that over 300 million surgical procedures are performed worldwide each year, with a risk of acute as well as long-lasting negative consequences [1]. One example is post-surgical pain that represents a significant burden to patients and, if insufficiently treated, can delay recovery, and may cause long-term effects [2–5]. Early consequences include an increased risk of complications after surgery, prolonged hospitalization, and the need for reoperation [2,3]. In the long-term, there is evidence for a high number of patients developing chronic postsurgical pain (CPSP) and opioid dependency. Both can limit the patient's quality of life and imposes a substantial socio-economic challenge for both patients and society [2,4,5]. The importance of CPSP was highlighted by its inclusion in the International Classification of Diseases catalogue (ICD-11th version, [6]). CPSP is defined as pain that persists after a surgical procedure beyond the healing process, i.e., for at least three months after surgery [6]. The prevalence of CPSP varies between studies mainly because most studies are mono-centric trials using different methodologies, endpoints, and definitions of CPSP. In the largest European multicenter, prospective, non-interventional trial on this topic, it has been shown that 41 % of all patients reported pain six months after surgery, with approximately 10 % having moderate-to-severe pain that impact their daily life [7]. Because treatment of CPSP is as intricate as other chronic pain states, prevention would be favorable. However, up to now, all drugs assessed for CPSP prevention failed [8]. One problem is the knowledge gap of mechanisms relevant for CPSP. As shown, the development of CPSP is multi-factorial and a complex bio-psycho-social contribution is most likely [4]. Furthermore, mechanisms of CPSP might even differ between patients and one treatment might not fit all. Thus, identifying these mechanisms and the factors responsible for the development of CPSP is of utmost importance for developing novel treatment strategies. Thus, pinpointing perioperative factors that positively (resilience factors) or negatively (risk factors) influence the development of CPSP, along with their relevance and interaction, appears to offer novel means of predicting patients at high risk [4,9,10]. However, none of the currently available "prognostic prediction models" are sufficiently effective [11], despite the fact that one of the most favorable model integrates a wide range of features, such as psycho-social and demographic ones [12,13]. Still, precision of prediction is only moderate as most likely it is missing important (e.g. biological) factors. Also, genetic factors failed to improve prediction within this model [13]. Remarkably, thus far, none of the prognostic prediction models have used unbiased proteomic analysis [14]; an unbiased proteomic approach might not only provide additional power to risk assessment but might also identify novel targets for treating CPSP.

Blood represents an easily obtainable diagnostic material in routine clinical practice. Blood plasma, with its diverse array of protein categorizations, including classical plasma proteins, tissue leakage proteins, and particularly signaling proteins such as hormones, growth factors, and cytokines, serves as a rich resource for modern biomarker discovery [15]. The presence and levels of these proteins may reflect the body's physiological and pathological states, making plasma an accessible window into overall health and disease mechanisms [16]. Consequently, analyzing blood plasma enables the identification of biomarkers for diagnosing diseases, monitoring health conditions, guiding therapeutic interventions, or prognosticating outcomes [17], underscoring its critical role in medical research and personalized medicine. Recent technological advances in sample collection and processing have promoted the detection of several hundred proteins in a single sample using mass spectrometry (MS). However, because of the wide dynamic range and fluctuating abundances of numerous proteins, plasma proteomics remains challenging [18]. Clinical laboratories often use highly optimized single-protein assays, allowing for a narrow/diagnostic snapshot while neglecting the complexity of (patho-)physiological conditions. In contrast, MS offers great potential for rapidly and robustly measuring several hundred proteins in a single human sample. Although MS approaches have not yet found their way into clinical routine guidelines, their versatile workflows, which allow for targeted as well as unbiased approaches, make them attractive for many clinical applications and research questions. To date, MS-based proteomics has been used in clinical settings in oncology, endocrinology, and rheumatology, supporting medical decision tools and providing profound knowledge of underlying molecular mechanisms[18–24].

We hypothesize that unbiased proteome analysis will enable identification of biological predictors associated with and likely relevant for the development of different phenotypes after an experimental incision as a model of acute postoperative and chronic pain. Furthermore, integrating psycho-physical and psycho-social features together with proteomic data from blood plasma could enable unprecedented performance in predicting post-surgical outcomes. To evaluate this in a standardized setting, we performed MS-based proteome analysis in a well characterized human experimental model for post-surgical pain [25,26], and combined this with psychological, psycho-physical and demographic phenotyping. We harnessed these data to determine multiple trait prognostic features under standardized experimental conditions and to develop prediction models for different phenotypes after experimental incision, in particular thosewith clinical relevance for postsurgical pain. Finally, by using an *in silico* drug repositioning approach, we identified drugs, which might revert the plasma protein signature identified in high pain responders.

2. Materials and methods

2.1. Study design

Upon recruitment, by notice boards at the university and medical campus Muenster, 26 male volunteers (age mean 23.9 $\pm$ SEM 3.6 years, Fig. 1A) gave written consent to be part of an incision-induced pain project after being informed about the study and experimental procedure. Informed consent was obtained from all participants prior to their inclusion in the study. All volunteers passed the listed in- and exclusion criteria in Supplementary material 1. Volunteers in this study were obliged to have an identical breakfast three days in a row. All human experiments were approved by the University Hospital Muenster of the local Ethics Committee of the Medical Faculty (registration no 2018–081-b-S), registered in German Clinical Trials Registry (DRKS-ID: DRKS00016641), in accordance with the latest version of the Declaration of Helsinki, and in line with the WHO Guiding Principles on Human Cell, Tissue and Organ Transplantation. Data from skin biopsies performed 24 hours after incision are included in a previous publication [27]. Comprehensive quantitative sensory testing, baseline psycho-social characterization, and blood sampling were performed before induction of incisional injury. An experimental incision was then made (Fig. 1B), and the incisional pain and hyperalgesic area were determined at fixed time points (Fig. 1C)

2.2. Chemicals and Reagents

Chemicals for an in-solution digest of plasma proteins were either purchased as a powder (ABC, IAA, SDC) or in liquid form (DTT, TCEP) from Merck Millipore/Sigma Aldrich (Germany). Protease for enzymatic digestion was a mixture of Trypsin/LysC, Mass Spec grade (Promega, USA). Ethyl acetate for surfactant removal was purchased from Merck Millipore/Supelco in hyper-grade purity (Lichrosolv). Acids for organic LC solvents or peptide clean-up were either purchased from Merck Millipore/Sigma Aldrich, Germany (TFA) or Thermo Scientifc, USA (FA). All MS-related solvents (water, ACN) were of hypergrade purity (Lichrosolv) and purchased at Merck Millipore (Supelco). C18 Micro-Spin columns (6–60 µg capacity) were supplied by The Nest Group (USA).
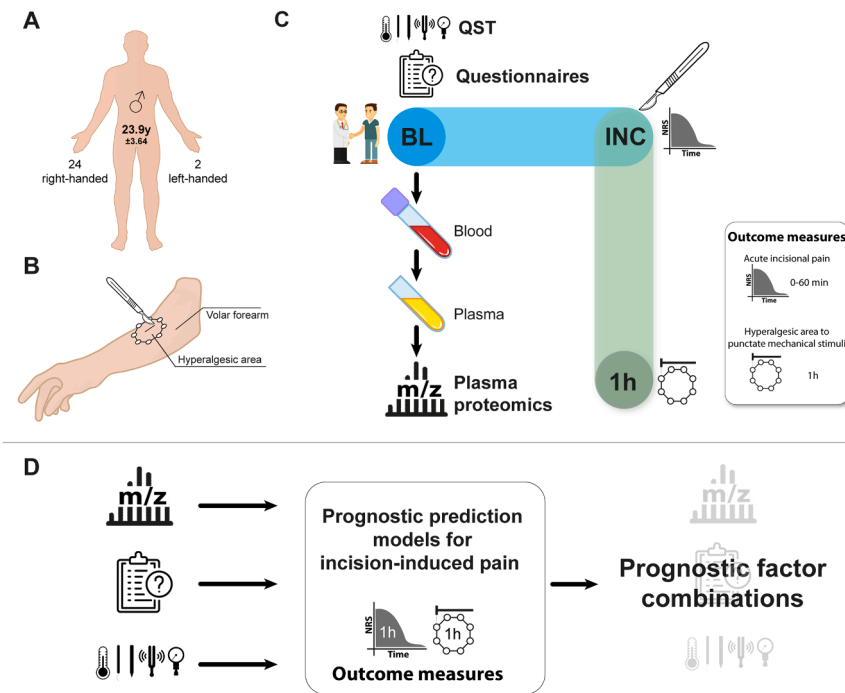
Fig. 1. Study design and methodology for predicting incisional outcome measures. (A) A total of 26 male volunteers (24 right-handed) with an average age of 23.9 years (y ± SD) were enrolled in the study. (B) Experimental incision (INC) was performed with a scalpel on the volar lower am (side randomized). The skin incision had 4 mm length and 7 mm depth. The secondary hyperalgesic area to punctate mechanical stimuli around the incisional injury was determined 1 h post incision. (C) Twenty-four h before incision (baseline, BL), the volunteer was medically briefed, complete qualitative sensory testing (QST) was performed in the incision area, five different questionnaires were completed, and blood was collected. Quantitative mass spectrometry was used to identify blood plasma proteome. (D) Analysis of BL's datasets allowed determination of the prognostic potential of single and combinatorial factors to predict pain phenotype, here, incisional pain graded on a numeric rating scale (NRS) and the dimension of the hyperalgesic area (HA) around the injury after incision.

2.3. Psycho-physical baseline characterization by quantitative sensory testing

Before incision, a comprehensive battery of quantitative sensory testing (QST) was performed on both forearms on the volar aspect (one forearm represents the test area where the incision will later be made, the other forearm represents the control side) to assess the perception of non-painful and painful stimuli of different modalities established by the German Research Network in Neuropathic Pain (DFNS) [28]. Testing is a subjective (psycho-physical) method requiring testing of person cooperation. Briefly, thermal testing will be performed by using a TSA-II NeuroSensory Analyzer (MEDOC, Ramat Yishai, Israel). With this device, thermal detection (warm, cold), pain thresholds (painful heat and cold), and pain to a defined suprathreshold painful stimulus will be determined [29]. The Advanced Thermal Stimulator thermode (contact area of 16 x 16 mm) was placed on the volar forearm. Testing starts at a neutral temperature (32°C) and increases (or decreases) with 1.5 °C/s up to a maximum of 50°C (or down to a minimum of 0°C). First, thresholds of cold (CDT) and warm (WDT) detection were measured three times each, followed by an assessment of pain cold (CPT) and heat (HPT) thresholds. Volunteers were instructed to press a button when sensation changes to warm/cold or become painful; then, the thermode immediately returns to the baseline temperature (32°C). If the cut-off temperature (50°C or 0°C) was reached, the device automatically returns to the baseline temperature (32°C) to avoid tissue damage. The mean value from the three measurements was taken as the heat and cold pain threshold. In addition, the pain intensity to a suprathreshold heat pain stimulus was assessed by application of three test stimuli (45, 46, and 47°C, using a ramp of 8 °C/s and time at the target of 7 s). In addition, subjects will be asked about paradoxical heat sensations (PHS) during the thermal sensory limen (TSL) procedure of alternating warm and cold stimuli. Modified von Frey filaments (OptiHair2-Set; Marstock

Nervtest, Schriesheim, Germany) that exert forces between 0.25 and 512 mN (geometric progression by factor 2) was used to assess the mechanical detection threshold (MDT). The end of the von Frey filaments was provided with a rounded tip (0.5 mm diameter) to avoid sharp edges that may activate nociceptors. Threshold determinations were made using an adaptive method of limits by a series of alternating ascending and descending stimulus intensities (up-and-downrule), yielding 5 just suprathreshold and 5 just subthreshold estimates. The geometric mean of these 10 determinations was represented the final threshold. Standardized punctate probes performed the assessment of mechanical pain sensitivity and threshold with fixed intensities (8, 16, 32, 64, 128, 256, and 512 mN), and a contact area of 0·2 mm diameter were used to determine mechanical pain sensitivity (MPS) and mechanical pain thresholds (MPT) [28,30]. Stimulators were applied at a rate of 2 s on, 2 s off in ascending order until the first percept of sharpness was reached to assess MPT. The final threshold was the geometric mean of five ascending and descending stimuli series. To determine MPS the same stimuli were applied in a pseudo-random order with a 10-sec interval in 5 runs; subjects were asked to give a pain rating for each stimulus on a '0–100' numerical rating scale ('0' indicating "no pain", and '100' indicating "most intense pain imaginable"). MPS was calculated as the geometric mean of all numerical ratings for each pinprick stimulus. QST parameters were measured in their physical dimension and were weighted by transformation to the standard normal distribution (Z-transformation). Z-scores indicate gain (above "0") or a loss (below "0") of function across QST-parameters.

2.4. Psycho-social baseline characterization by patient-reported outcome measures (PROMs)

Prior incision injury, volunteers have completed a set of psychological questionnaires, including the Beck-Depressions-Inventar 2 (BDI-2),

the state-trait anxiety inventory (STAI), the pain catastrophizing scale (PCS), the Life Orientation Test - Revised (LOT-R), and the pain sensitivity questionnaire (PSQ) to identify possible risk factors for incision-induced pain. PSQ is a self-rating instrument for the assessment of pain sensitivity, validated in healthy subjects and chronic pain patients [31–35]. The volunteer completed the questionnaires himself in a quiet neutral room in the presence of a male experimenter. The order of the questionnaires was randomized a priori by an Excel list for each volunteer individually.

2.5. Blood sampling and plasma processing

Blood samples (5 ml) were collected by venipuncture of the contralateral arm under sterile conditions. Winged blood collection sets (BD Vactuainer® Safety-Lok™, needle gauge 21) were used to collect the blood in EDTA tubes (BD Vactuainer®, K2EDTA, 1·8 mg/ml). All tubes were gently rotated eight times by hand after sampling. Blood cells, including platelets, were removed from plasma by centrifugation at 2000 x g for 15 minutes in a refrigerated centrifuge (4°C) to obtain blood plasma samples. The blood plasma was divided into 0.5 ml aliquots and stored at −20 °C.

2.6. Experimental incision

The experimental incision followed a protocol previously described [26,30,36]. Briefly, the skin of one randomly chosen arm for incision was disinfected with 70 % ethanol. An incision of 4 mm width and 7 mm depth was 'applied' with a sterile scalpel (No. 11), perforating the muscular fascia. A gauze swab stopped the bleeding of the wound with gentle pressing (Fig. 1B).

2.7. Determination of incisional pain and hyperalgesic area as outcome measures

Two outcome measures were defined as clinical relevant measures translating well to patients after surgery. First, volunteers were asked to rate incision-induced pain intensity (IncP) on a numeric rating scale (NRS, 0–100) at time zero (during incision), every minute until 10 minutes, every five minutes until 1 hour after incision. The area under the curve (AUC) was determined for the first 60 minutes after incision, which represents acute incisional pain. This refers well to acute postsurgical pain intensity, a measure that is one primary outcome parameter to be assessed in clinical trials related to postsurgical pain [37]. Second, sensitivity to punctuate mechanical stimulation in the zone around the incision, namely the hyperalgesic area (HA), was determined 60 min post-incision using a conventional von Frey filament with 116 mN bending force. It was applied in eight imaginary lines at 45°, starting far distant from the putative hypersensitivity region centripetally directed towards the incision. All eight points were linked, transferred onto a paper, and the area was determined in Image J (https://imagej.nih.gov/ij/). As a proxy of central sensitization, the area of hyperalgesia surrounding the surgical incision in patients has been shown as a consistent predictor of CPSP in clinical studies [38–40] and was used to estimate preventive efficacy of treatments for CPSP [41].

2.8. Definition of responders for incision-induce outcome measures

Volunteers were stratified into responder types depending on the IncP and the extent of the HA. The mean of the entire cohort was calculated for both outcome measures. Being above or below the corresponding mean, volunteers were stratified into high (> mean) and low (< mean) responders, In the following, volunteers with a larger IncP (above the mean) and larger HAs (above the mean) are designated as high responders. Ultimately, we defined IncP and HA as reference parameters for psycho-physical, psychometric, and proteomic analyzes to determine incision injury single marker and multi-feature prediction signatures.

2.9. Sample preparation: protein digestion and sample clean-up

Plasma samples were neither fractionated nor depleted. Plasma samples were allowed to thaw on ice and sonicated in 15 s intervals, depending on the degree of denatured components. 10 µL plasma, corresponding on average to 36,1 µg/µL were diluted in 5 mM TCEP, 1 % SDC in 100 mM ABC (DR buffer). Samples were denatured and reduced for 1 h at 60°C with agitation in a thermoshaker. 15 µL of the denatured mixture was further diluted with 100 mM ABC in a 1:1 ratio and alkylated with 10 mM IAA at room temperature for 30 min (in the dark). Quenching of samples was obtained by adding 10 mM DTT final for 15 min of incubation at room temperature. Samples were diluted with MS-grade H_2O to perform protein hydrolysis in 50 mM ABC at pH 7,8 – 8,0. Tryp/rLys-C was added 1:50 (enzyme: protein) and incubated overnight (16 hours) at 37°C using a heated thermoshaker with heatable lid (40°C) to prevent condensation within the Eppendorf tube.

Removal of detergents was obtained by phase transfer following the protocol by Masuda and Ishihama [42]. After discarding the surfactant-containing upper layer, the remaining peptides were desalted using solid-phase extraction (SPE). C18 MicroSpin (The Nest Group, USA) columns were used for SPE, adhering to the manufacturer's instructions with the following modifications: bound peptides were sub-sequentially washed with 0.5 % TFA and 0.2 % TFA, two-step elution of peptides with 50 µL 50 % ACN, 0.1 % FA and 50 µL 80 % ACN, 0.1 % FA. Cleaned-up peptides were fully dried using a vacuum evaporator at 38°C.

2.10. Liquid chromatography and mass spectrometry

Dried peptide samples were solubilized in MS buffer (1 % ACN, 0.1 % FA) and sonicated for 2 min. Peptide concentrations were determined using a UV/VIS Spectrometer at 280 nm/430 nm (IMPLEN, Germany). Autosampler vials contained 100 ng/µL sample and iRT (Biognosys, Switzerland) peptides for prediction of peptide retention times upon chromatographic separation [43]. A pooled sample of V1-V3 (100 ng/µL) was run before each acquisition queue to control for consistent system performance.

NanoLC-MS/MS analyzes were conducted on an Orbitrap Exploris 480 mass spectrometer coupled with an UltiMate 3000 UHPLC System (Thermo Scientific, Germany). In a direct setup, 2 µL peptides were separated on an Acclaim PepMap column (75 µm x 15 cm, C18, 2 µm, 100 Å) at a constant flow rate of 300 nl/min and injected to the mass spectrometer via a Nanospray FlexTM ion source (Thermo Scientific, USA). The mobile phase consisted of [A] 0.1 % FA, 1 % ACN and [B] 0.1 % FA, 100 % ACN. MS acquisition included peptides eluting along a two-step linear gradient of 3–25 % B in 60 min and 25–40 % B in 20 min. The high organic phase (80 % B, 10 min) and two subsequent short gradients (3–50 % B 10 min; 80 % B 4 min) within the same injection cycle were without MS acquisition to ensure minimization of a column-and LC system-related carryover in a time-efficient manner. The column temperature was set to 40°C constantly. MS raw data were acquired in data-independent acquisition mode (DIA) in a scan range of 350–1154 m/z. MS1 spectra were recorded at a resolution of 120,000 and automatic gain control (AGC) target of 3e6 or 60 ms injection time, respectively. Corresponding MS2 scans were acquired at 30,000 resolutions with an AGC value of 3e6 and auto for injection time. Each DIA segment contained 15 spectra of 18 Da windows with a stepped collision energy of 25, 27, and 30. A total of three full scans, each followed by symmetrically segmented isolation windows, was needed to cover the entire MS scan range. All spectra were recorded in profile mode.

2.11. Quantitative LC-MS data analysis

The raw DIA data files were processed with the open source program

DIA-NN 1.8.1 [44]. As a spectral library, an in-house library stemming from human plasma depletion experiments was used. The spectral library contained 4590 protein isoforms, 2889 protein groups and 17809 precursors in 14923 elution groups. For the in vitro digestion, Trypsin/P was chosen and a maximum of three missed cleavages. Peptide length was set to 5–52 amino acids. Cysteine carbamidomethylation was chosen as a fixed modification and as possible variable modifications N-term methionine excision, methionine oxidation, and/or N-term acetylation were set. The maximum number of variable modifications allowed was 3. RT-dependent cross-run normalization and Robust LC (high accuracy) options were selected for quantification. The R package, DiaNN (https://github.com/vdemichev/diann-rpackage; [44]) was used to extract the MaxLFQ [45] quantitative intensity of protein groups for all identified protein groups with q-value < 0.01 as criteria at precursor and protein group levels. Due to poor data quality, V7 was excluded from all analyzes. All raw data files have been uploaded to the Proteome Xchange Consortium[46] via the PRIDE partner repository with the dataset identifier PXD033592. Whenever a protein group had several proteins mapped, only the first mapped protein of each protein group was considered in all analyses downstream of the ROC analysis.

Blood collection and subsequent variations in sample handling and processing can lead to contamination of plasma. Geyer et al., 2019, investigated this issue systematically, and reported proteomic catalogs of contaminating cell types, namely erythrocytes, platelets as well as coagulation events [47]. We compared our identified and quantified protein groups with their so called "quality marker panels" and found 58 putative contaminants. We did not exclude those per se from the ROC analysis as Geyer et al. reported that several of these proteins were still identified in pure plasma indicating a baseline level of contaminants due to imperfect de-enrichment or the life cycle of these cells. Instead, we excluded them only from downstream analyses after the ROC analysis, e.g., the Cytoscape, PharmOmics, and Interactome analysis. Any detected keratins (11 protein groups) were also excluded from mentioned downstream analyses.

2.12. Statistical analyzes, bioinformatic processing, and post-hoc analyzes

Feature-selection of prognostic marker and marker combinations was performed in the statistical environment R. If not reported otherwise, data were analyzed using OriginLab PRO.

2.12.1. Functional analysis

Functional enrichment analysis of all 383 identified and quantified proteins at high confidence (0.7) was performed using the web-based STRING interface (https://string-db.org/ [48], analysis was performed on 23/02/2024).

2.12.2. Network analysis

Cytoscape (version 3.8.2, available at cytoscape.org) [49] was used to identify pain phenotype-specific protein networks (term-term-interactions (TTI)-networks). Functional grouping within these networks was achieved using AutoAnnotate version 1.3. Analysis revealed significantly enriched GO terms (p-values ≤ 0.05) within these functionally grouped networks, effectively reflecting the relationships between these terms.

2.12.3. Network-based drug repositioning with PharmOmics

The network-based repositioning tool within the open-source application PharmOmics (http://mergeomics.research.idre.ucla.edu/runpharmomics.php) [50] was used. As input genes, the high responder prognostic markers were taken. The analysis was run for both outcome measures (IncP, HA) separately. The signature type was set to "Meta", species to "Human" and as the background network we chose (i) "Sample Multi-tissue Network" (provided by PharmOmics) and (ii) a protein-protein interaction network created with STRING (https://string-db.org/) [48], analysis performed in January 2024) based on our own identified plasma proteins (yielding a network with 285 nodes). The output was filtered for the tissues "hematopoietic system" and "immune system".

2.12.4. Interactome analysis

To detect potential interactions between our high responder prognostic markers with proteins expressed by human nociceptors, we used a curated ligand-receptor database via the web application https://sensoryomics.shinyapps.io/Interactome/ [51]. The chosen dataset was "human_DRG_integrated" which is based on [52,53].

2.12.5. Logistic regression analyzes

This study aimed to propose prognostic prediction models for the pre-defined outcomes measures (IncP, and HA, Fig. 1D). Therefore, we employed logistic regression models in R to identify combinations of available candidates (i.e. covariates) that correlate with a high probability for high responders. We developed an analysis pipeline comprising the following steps: (I) data pre-processing, (II) model building, and (III) evaluation of model robustness. Data pre-processing applies normalization per candidate and a linear shift to a beneficial data range for subsequent analysis. This data shift is introduced only for technical reasons and alters data in any relevant manner. Then, the normalized and shifted predictors are analyzed using the combiroc package[54]. A wrapper function has been programmed which allows to firstly analyze each candidate variable individually, filter predictors for a selected minimal AUC value and subsequently evaluate all combinations between all selected candidates. All models are fitted according to the comibroc default procedure, i.e. to fit logistic regression models. All combinations generated in step II are evaluated by leave-one-out cross-validation (LOOCV). We defined deviance measures by calculating the mean squared difference between the AUC from all volunteers and the individual LOOCV AUCs. We used the overall AUC and its deviance to rank each predictor or combination. The selection of the optimal predictor/combination is a multi-criteria optimization problem (maximize AUC & minimize deviance). Thus, more than one combination could be optimal in the sense of a Pareto front. In this case, an expert decision has been applied based on other criteria, e.g. applicability or feasibility of the specific measures in the clinical context. Our pipeline also allows restricting the search space to pre-specified subsets of combinations - e.g., we can restrict the algorithm to search within all combinations of maximal length three and pre-specify that each candidate shall be of a distinct dimension (e.g. 1x psycho-physical parameter + 1x psychological parameter + 1x blood plasma protein). The receiver operator curves (ROC) of the fitted logistic regression models yield AUC values.

3. Results

3.1. Volunteer characterization through pre-incisional sensory phenotyping, psychological profiling, and plasma proteome analysis

A cohort of 26 male volunteers, with a mean age of 23.9 years (SD, ± 3.64), was enrolled in the study with specific inclusion and exclusion criteria (Fig. 1A; Supplementary material 1). Baseline (BL) characterization was performed to assess potential prediction of post-incisional outcome parameters with psycho-physical assessments (QST) and psychological patient-reported outcome measures (PROMs). The results of the QST suggest a sensory profile that is non-pathological, with slight differences observed between the control and test regions (Fig. 2A, Supplementary material 2). Cold and warm detection thresholds were (mean ± SD) $-1.32 \pm 0.53°C$ vs. $-1.53 \pm 0.92°C$ (CDT) and $2 \pm 0.86°C$ vs. $2.2 \pm 0.69°C$ (WDT). Pain thresholds showed similar trends, with CPT at $-13.38 \pm 7.6°C$ (control) and $-11.83 \pm 8.49°C$ (test), and HPT at $9.88 \pm 3.9°C$ vs. $10.20 \pm 3.43°C$. Mechanical thresholds were comparable, with MDT at 1.33 ± 1.53 mN vs. 1.23 ± 1.36 mN, and MPT at
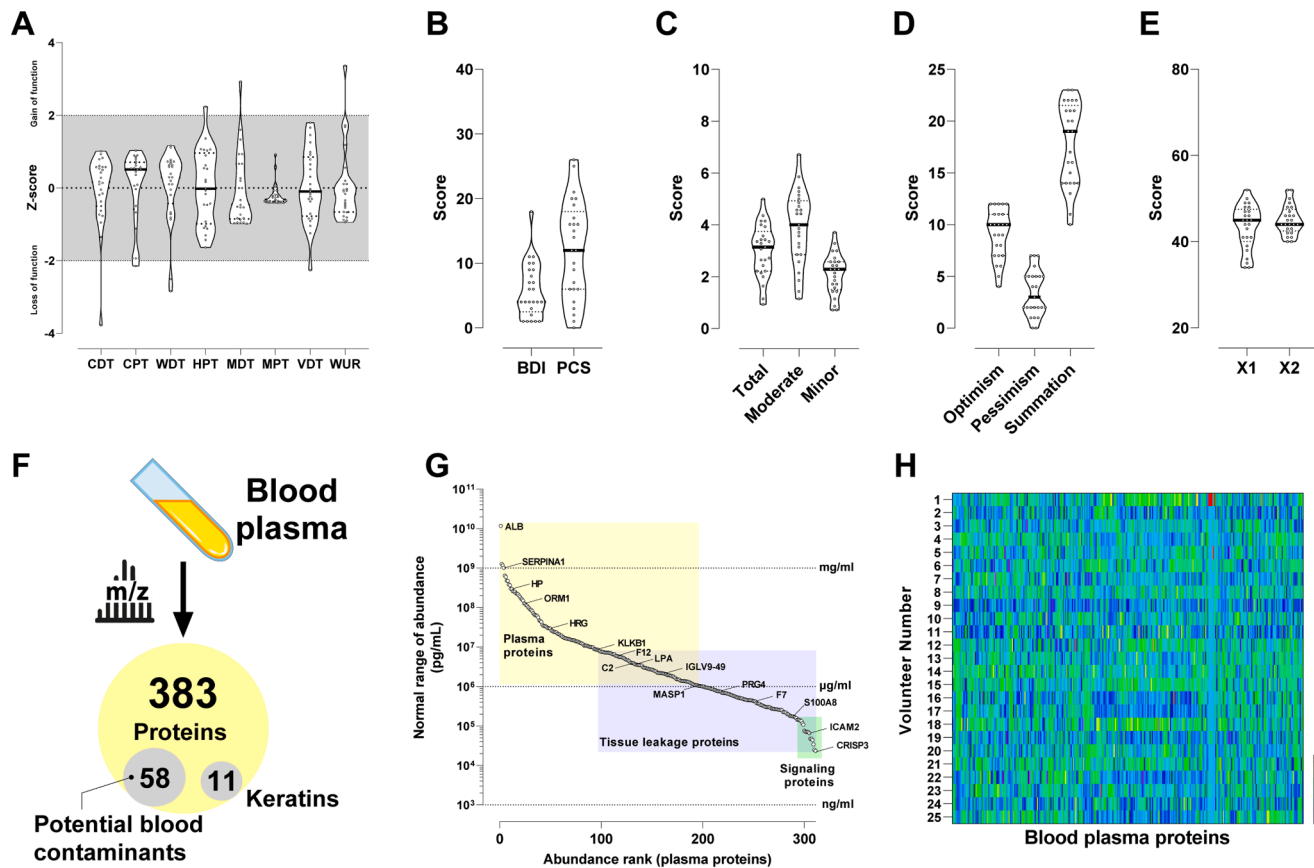
Fig. 2. Pre-incisional psycho-physical phenotyping, psycho-social characterization and unbiased proteome profiling of blood plasma proteins in male volunteers. (A) Detection of pre-incisional somatosensory perception to natural stimuli (thermal and mechanical) was achieved by a complete quantitative sensory testing (QST) battery on both forearms. The contralateral forearm served as the control side. Z-scores above '0' show a gain of function (more sensitive) and below a loss of function (less sensitive). Values above or below two-fold standard deviation (SD, dotted line) show pathological QST-scores, (Violin Plots, Median ± 95 % CI). Abbreviations: CDT, cold detection threshold; CPT, cold pain threshold; HPT, heat pain threshold; MDT, mechanical detection threshold; MPS, mechanical pain sensitivity; MPT, mechanical pain threshold; PPT, pressure pain threshold; TSL, thermal sensory limen; VDT, vibration detection threshold; WDT, warmth detection threshold; WUR, wind-up ratio. (B) The individual distribution of the Beck Depression Inventory (BDI) and Pain Catastrophizing Scale (PCS) scores are shown, which illustrate the psychological profiles of the study participants regarding depression and pain catastrophizing, (Violin Plots, Median ± 95 % CI). (C) The individual distribution of the Pain Sensitivity Questionnaire (PSQ-Total, Moderate, and Minor) scores are shown, which illustrate the psychological profiles of the study participants regarding stress perception (Violin Plots, Median ± 95 % CI). (D) Individual scores of the Life Orientation Test (LOT-Optimism, LOT-Pessimism, and LOT Summation) scores, illustrating the psychological profiles of the study participants in terms of optimism and pessimism, (Violin Plots, Median ± 95 % CI). (E) Individual distribution of the State-Trait Anxiety Inventory (STAI X1, X2) scores, illustrating the psychological profiles of the study participants in terms of anxiety levels, (Violin Plots, Median ± 95 % CI). (F) Identification and quantification of 383 pre-incisional blood plasma proteins. When comparing the 383 proteins with quality marker panels for blood plasma samples, 58 assumed contaminations and 11 keratins were found. (G) UniProtKB keyword annotations and their enrichment across the protein abundance spectrum. Exemplary proteins contributing to keywords are highlighted in red. ALB, albumin; SERPINA1, serpin family A member 1; HP, haptoglobin, ORM1, alpha-1-acid glycoprotein 1; HRG, histidine-rich glycoprotein; KLKB1, plasma kallikrein; F12, coagulation factor XII; C2, complement C2; IGLV9–49, Immunoglobulin Lambda Variable 9–49; MASP1, Mannan-binding lectin serine protease 1; F7, coagulation factor VII; S100A8, S100 calcium binding protein A8; ICAM2, Intercellular adhesion molecule 2; CRISP3, Cysteine Rich Secretory Protein 3. (H) The heatmaps show z-weighted median intensities of the 383 quantified plasma proteins for each of the 25 volunteers.

55.82 ± 32.11 mN vs. 74.4 ± 142.88 mN.

The pre-incisional PROMs data show that the experimental cohort exhibits a psychological and pain sensitivity profile that is clinically inconspicuous (Fig. 2B-E, Supplementary material 3). The BDI-2 score was 4 (median) [95 % CI, 4–7.3], within the "clinically unremarkable" range. Optimism and pessimism scores from the LOT-R Test were 10 [8.2–10.1] and 9 [7.8–9.5], respectively, also clinically unremarkable. Within the range of 16.2–19.3, the total LOT-R score was 19. No significant catastrophizing was showed by a PCS score of 12 [9.1–14.9]. The PSQ yielded minor, moderate, and total scores of 2.2 [1.8–2.4], 3.9 [3.3–4.4], and 3.1 [2.6–3.4], all within normal limits. The STAI scores for State (X1) and Trait (X2) were 34 [31.3–36.1] and 35 [33.4–39.6], showing no significant anxiety symptoms. Considering our quality and cut-off criteria (please see methods for details), we identified and quantified 383 protein groups (hereafter coined "proteins") across

samples (Fig. 2F-H, Supplementary material 4; Supplementary Table 1). Out of the total 383 protein, 58 were identified as potential blood contaminants [47] and 11 were keratins. Due to inadequately high lipid concentration in the blood plasma, one volunteer was excluded from all subsequent analyzes. In accordance with the Human Protein Atlas (https://www.proteinatlas.org/humanproteome/), identified proteins could be categorized into *blood plasma proteins, tissue leakage proteins,* and *signal proteins,* like cytokines or hormones usually found in the low concentration range (Fig. 4G). To gain more insights into the predicted function of quantified proteins, we performed Gene Ontology (GO) enrichment analysis and REACTOME pathway analysis using the STRING web interface (please see methods for additional details; Supplementary material 4; Supplementary Table 1). As expected, a significant portion of the top results were associated with their role in oxygen and nutrient transportation, immune response, and blood clotting.

3.2. Determination of primary outcome measures after incision injury

Up to one hour after the experimental incision injury, both outcome measures were assessed. The intensity of IncP was highest at the time of incision and declined rapidly within the first ten minutes (Supplementary material 5). Integration of the AUC for each volunteer's NRS values provided individualized NRS_{AUC} values, showing a significant reduction in IncP over time (***P < 0.001). HA was determined in response to punctate mechanical stimuli one hour after incision, revealing an average size of 68.65 cm^2 (SD, ± 50.9) across the cohort (Supplementary material 5).

3.3. Predictive modeling of post-incisional outcome measures using integrated pre-incisional multi-modal features

Using the IncP as primary outcome, stratification of the volunteers resulted in 9 individuals classified as high responders (with a range of 36.1–458.5) and 16 individuals classified as low responders (with a range of 1.7–30) (Fig. 3A). By evaluating individual pre-incisional multi-modal features and incorporating them, we created prognostic predictive models for this outcome measure. Prognostic proteome signatures were ranked and selected using logistic regression analysis, revealing the best performing proteins. ROC-curves and the corresponding AUC (ROC_{AUC}) determined features for either high- (ROC_{AUC} ↑) or low responders (ROC_{AUC} ↓) for proteome, psycho-physical parameters, and multiple-construct psychological profile. To sum up, among the 383

blood plasma proteins that were identified, 70 proteins displayed an $ROC_{AUC} > 0.6$, while 72 proteins showed an $ROC_{AUC} < -0.6$ (Fig. 3B, Table 1) for IncP across all protein categories. QST parameters, such as CPT and WUR were determined to be features for high responders, while the (MDT was observed to be linked with low responders (Fig. 3C). Stress, as measured by the PSQ in both total and moderate forms, was used as a feature to identify high responders (elevated) among psychological metrics (Fig. 3D). On the other hand, the evaluation of dispositional optimism at the individual level, as measured by the LOT, served as a feature for individuals with low responses (↓) (Fig. 3D).

Following an analysis of the outcome measure HA, we determined 12 volunteers as high responders, displaying a HA range of 63.5–184 cm^2. Furthermore, 13 individuals were identified as low responders, exhibiting a range of 1–63.5 cm^2 (Fig. 3E). Interestingly, on the proteome level, 60 proteins exhibited an ROC_{AUC} value greater than 0.6 for HA. Additionally, 55 proteins were characterized by an ROC_{AUC} value lower than -0.6 (Fig. 3F, Table 2), again in all protein categories. The prognostic QST parameters for individuals classified as high responders were determined to be the WDT, HPT, MDT, VDT, and WUR (Fig. 3G). PROMs for depression (BDI-2), PCS, LOT, and PSQ-Minor served as indicators for identifying individuals classified as high Responders for HA (Fig. 3H).

By employing data-driven prognostic predictive models of two or three QST parameters, there was a slight elevation in the mean ROC_{AUC} for IncP from 0.62 [0.43–0.73] to 0.67 [0.38–0.76], ∆AUC= 0.05), as opposed to using only one parameter (0.53 [0.37–0.79]) (Fig. 4A,
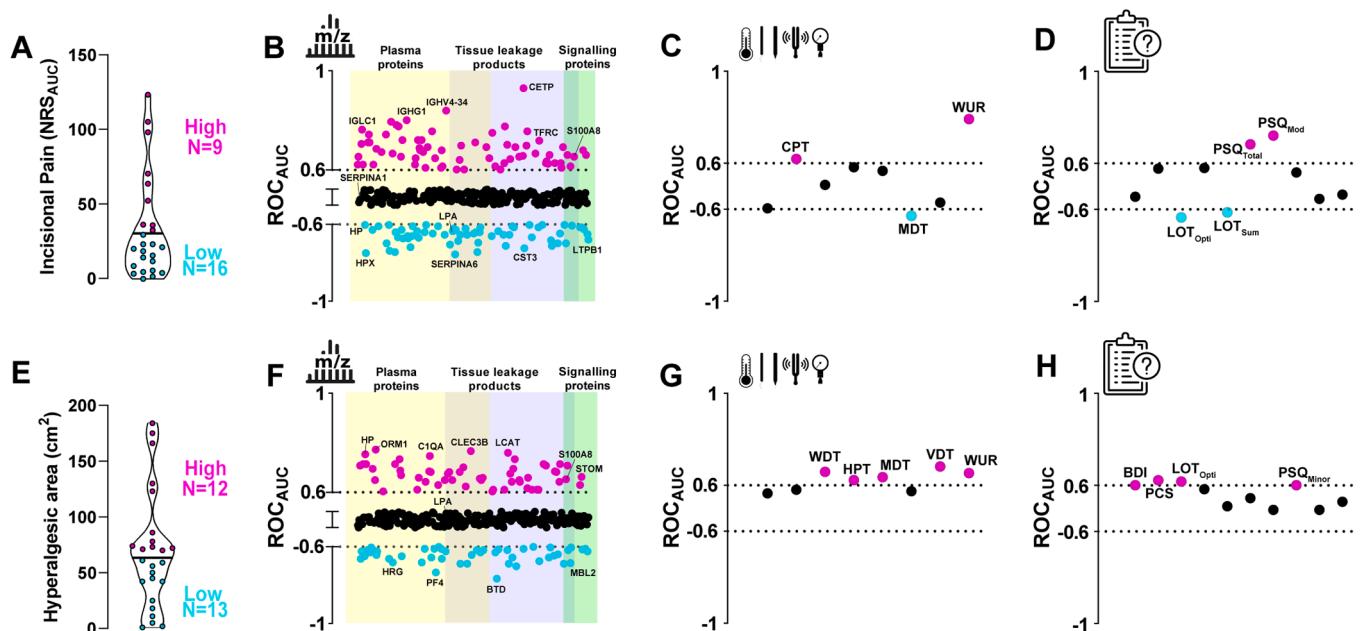

Fig. 3. Prognostic value of pre-incisional blood plasma proteome profile, psycho-physics, and psycho-social phenotype for post-incisional outcome measures. (A) Volunteers were asked to judge the ongoing pain caused by the incision using the Numeric Rating Scale (NRS; 1–100). Integrated data from the first hour after the incision were analyzed, and the area under the curve (AUC) were plotted. Twenty-five volunteers were stratified into low (N = 16;) or high (N = 9) responders depending on pain ratings. (B) Prognostic value of each of 383 pre-incisional blood plasma proteins for high (70 proteins) and low responders (72 proteins) for incisional pain. (C) Prognostic value of all parameters of psychophysical testing for high (CPT and WUR) and low responders (MDT) for incisional pain. (D) Prognostic value of PROMs for high (PSQ-Total, PSQ-Moderate) and low responders (LOT-Optimism, LOT-Summation) for incisional pain. (E) Upon incision injury, hyperalgesic area (HA) was assessed post 1 h (HA) in 25 volunteers. Phenotyping was achieved by determining the total cohort's mean HA (68.65 cm^2). Volunteers with a lower HA were categorized as "low responders" (N = 13), and those with higher mean as "high responders" (N = 12). (F) Prognostic value of each of 383 pre-incisional blood plasma proteins for high (60 proteins) and low responders (55 proteins) for hyperalgesic area post-incision (HA). (G) Prognostic value of all parameters of psycho-physical testing for high (WDT, HPT, MDT, VDT, WUR) for HA. (H) Prognostic value of PROMs for high (BDI, PCS, LOT-Optimism, and PSQ-Minor) for HA. Abbreviations: CDT, cold detection threshold; CPT, cold pain threshold; HPT, heat pain threshold; MDT, mechanical detection threshold; MPS, mechanical pain sensitivity; MPT, mechanical pain threshold; PPT, pressure pain threshold; TSL, thermal sensory limen; VDT, vibration detection threshold; WDT, warmth detection threshold; WUR, wind-up ratio; BDI, Beck Depression Inventory; PCS, Pain Catastrophizing Scale; PSQ-Total, Pain Sensitivity Questionnaire-Total; PSQ-Moderate, Pain Sensitivity Questionnaire-Moderate; PSQ-Minor, Pain Sensitivity Questionnaire-Minor; LOT-Optimism, Life Orientation Test-Optimism; LOT-Pessimism, Life Orientation Test-Pessimism; LOT Summation, Life Orientation Test Summation; STAI x1, State-Trait Anxiety Inventory Form X1; STAI x2, State-Trait Anxiety Inventory Form X2.

Table 1

Predictive value for pre-incisional blood plasma proteines (**only proteins > I0.6I ROC_{AUC} were considered**) for the outcome measure IncP.

Protein	ROC_{AUC}
CETP	0.93
IGHV4-34	0.84
IGHG1_IGHG2	0.80
IGKV3-20_IGKV3D-20	0.79
JCHAIN	0.78
IGHG1_IGHG4	0.78
IGLV1-36	0.78
IGLC7_IGLL5	0.76
IGHD	0.76
IGHV4-4	0.76
IGLV1-51	0.75
IGKV3-11	0.74
IGLC7	0.74
IGKV1-27_IGKV1-8	0.72
IGKV2-40_IGKV2D-40	0.72
IGKV3D-20	0.72
TGFBI	0.72
IGHA1	0.71
IGHG1_IGHG3_IGHG4	0.71
IGLV2-14	0.71
IGKC	0.71
IGHV4-28	0.70
FCGBP	0.70
IGKV1-39_IGKV1D-39	0.70
IGHV3-23_IGHV3-74	0.69
IGHV3-38	0.69
IGLV3-21	0.69
NRP1	0.69
IGLV1-44_IGLV1-47	0.69
IGKV3-7	0.69
C7	0.68
ICAM2	0.68
IGHV4-34_IGHV4-4	0.68
IGKV3D-15	0.68
IGLL5	0.67
KIF20B	0.67
HRG	0.67
IGLV3-19	0.67
IGLV3-25_IGLV3-27	0.66
KRT2_KRT5	0.66
SAA1	0.66
IGHV3-33	0.66
IGHG1	0.65
IGHV1-2	0.65
IGKV1-33_IGKV1D-33	0.65
QSOX1	0.65
IGHV3-13_IGHV3-20_IGHV3-43_IGHV3-7	0.65
IGLV1-44	0.65
LYZ	0.65
KRT9	0.64
C8G	0.64
ANG	0.63
CFHR5	0.63
IGHV1-3	0.63
IGKV1D-8	0.63
IGLV3-21_IGLV3-9	0.63
IGLV3-10_IGLV3-25	0.63
ALB	0.62
IGKV3-20	0.62
ITIH3	0.62
TFRC	0.62
GP1BB	0.62
IGKV2-30	0.62
MINPP1	0.62
IGKV4-1	0.61
IGLV1-40	0.61
LRG1	0.61
APMAP	0.60
FBLN1	0.60
IGLV2-8	0.60
SERPINA7	−0.76
HPX	−0.75
CFH	−0.74

(continued on next page)

Table 1 (*continued*)

Protein	ROC_{AUC}
SELENOP	−0.74
APOM	−0.74
CST3	−0.72
APOC1	−0.72
PCYOX1	−0.71
RBP4	−0.71
C1R	−0.71
APOA4	−0.70
FCGR3A	−0.70
MST1	−0.70
PEPD	−0.70
DBH	−0.70
ITIH4	−0.69
APCS	−0.68
LUM	−0.68
C1QC	−0.67
SERPING1	−0.67
PI16	−0.67
APOC3	−0.67
KLKB1	−0.67
SAA4	−0.67
APOD	−0.66
AZGP1	−0.66
IGKV1-17	−0.66
APOA2	−0.65
APOC4	−0.65
ATRN	−0.65
CFI	−0.65
LPA	−0.65
MASP1	−0.65
CRISP3	−0.65
CFHR2	−0.65
F2	−0.65
ORM1	−0.65
SERPINF2	−0.65
APOC2	−0.64
F10	−0.64
FN1	−0.64
IGHV5-51	−0.64
C6	−0.63
PTGDS	−0.63
S100A8	−0.63
APOE	−0.63
C1S	−0.63
HP_HPR	−0.63
LPA_PLG	−0.63
ANPEP	−0.63
C2	−0.62
F13B	−0.62
BCHE	−0.62
HABP2	−0.62
PLG	−0.62
PROS1	−0.62
PTPRJ	−0.62
TF	−0.62
C5	−0.61
GC	−0.61
HBB	−0.61
HBB_HBD	−0.61
IGF2	−0.61
CA2	−0.61
S100A9	−0.61
CFHR1	−0.60
ENO1	−0.60
F11	−0.60
HP	−0.60
IGHG2_IGHG3	−0.60
IGHV3-7	−0.60
SERPINA1	−0.60

Supplementary material 6). A similar picture can be witnessed with PROMS (Fig. 4A). Similarly, integrating 2 (0.67 [0.43–0.83]) or 3 (0.66 [0.42–0.76]) PROMs also led to an increase in accuracy for IncP (Supplementary material 7). The prognostic value for IncP does not become more accurate by combining a QST parameter and a PROM

Table 2

Predictive value for pre-incisional blood plasma proteines (**only proteins > I0.6I ROC$_{AUC}$ were considered**) for the outcome measure HA.

Protein	ROC$_{AUC}$
ORM1_ORM2	0.77
CLEC3B	0.77
FGA	0.77
LCP1	0.76
HP	0.75
C1QA	0.75
C9	0.73
F9	0.73
C1S	0.73
CFH	0.71
HPX	0.71
LBP	0.71
ORM1	0.71
TFRC	0.71
CFHR5	0.71
FGG	0.71
KRT2_KRT5	0.71
SERPINA10	0.71
C1QB	0.70
HP_HPR	0.69
SERPINA3	0.69
ORM2	0.69
IGKV1D-8	0.69
KRT1	0.69
C4B	0.68
C8G	0.68
PRG4	0.68
SERPIND1	0.68
C8B	0.68
KRT9	0.68
IGKV1-33_IGKV1D-33	0.67
TF	0.66
KRT10	0.66
KRT2	0.66
PI16	0.66
F10	0.66
PEPD	0.65
APOL1	0.65
CFI	0.65
CPB2	0.65
IGHV1-2	0.65
PCOLCE	0.65
IGLV1-40	0.64
IGLV4-69	0.64
LGALS3BP	0.64
MBL2	0.64
C5	0.63
CAT	0.63
FGB	0.63
PLG	0.63
F13B	0.62
IGHV4-4	0.62
CFP	0.61
IGLV3-21_IGLV3-9	0.61
KRT83_KRT86	0.61
PROS1	0.61
S100A8	0.61
SAA4	0.61
CP	0.60
IGLV1-51	0.60
APOC3	−0.78
BTD	−0.77
PGLYRP2	−0.73
IGLL1	−0.70
ATRN	−0.69
IGHV3-43D	−0.69
LPA	−0.69
SHBG	−0.69
MINPP1	−0.69
HRG	−0.68
IGKV2-40_IGKV2D-40	−0.68
TGFBI	−0.68

Table 2 (*continued*)

Protein	ROC$_{AUC}$
C7	−0.66
IGHG1_IGHG2_IGHG3_IGHG4	−0.66
IGHG2_IGHG3	−0.66
C4A	−0.66
IGF2	−0.66
SELL	−0.66
APOE	−0.65
IGHG2	−0.65
SERPINA5	−0.65
GP1BA	−0.65
MSN	−0.65
IGFBP3	−0.64
IGKV3-7	−0.64
FCGR3A	−0.64
GP1BB	−0.63
HABP2	−0.63
IGHA1	−0.63
IGHA1_IGHA2	−0.63
A2M_PZP	−0.62
CRISP3	−0.62
IGKC	−0.62
IGKV2-24_IGKV2D-24	−0.62
TUBB4B	−0.62
CORO1A	−0.62
IGHG2_IGHG3_IGHG4	−0.62
IGHV1-18	−0.62
IGHV4-28	−0.62
IGLV2-18	−0.62
HSPA1A_HSPA1B_HSPA1L	−0.61
PTGDS	−0.61
ADAMTS13	−0.61
APOC2	−0.61
CETP	−0.61
IGFALS	−0.61
IGHG1_IGHG3	−0.61
IGKV4-1	−0.61
A2M	−0.60
BCHE	−0.60
HSPB1	−0.60
IGHV3-13	−0.60
CRTAC1	−0.60
IGHV3-49	−0.60
PARVB	−0.60

(0.63 [0.42–0.83], Fig. 4A, Supplementary material 8). The prognostic values of QST (Supplementary material 9), PROMS (Supplementary material 10), and the combined use of both for the outcome parameter HA showed a comparable pattern (Fig. 4B). The model's accuracy in this scenario was 0.62 [0.49–0.78] (Fig. 4B, Supplementary material 11).

In contrast, data-driven prognostic predictive models of 2 or 3 proteins resulted in improved accuracy for both outcome measures, with a mean value of 0.81 [0.67–0.99, ΔAUC= 0.13] for IncP (Fig. 4A, Supplementary material 12, 13) and 0.85 [0.7–0.96, ΔAUC= 0.13] for HA (Fig. 4B, Supplementary material 14, 15), when compared to the utilization of only one protein. Prognostic predictive models, including a protein and a QST parameter or a protein and a PROM did not increase the mean accuracy for both outcome measures compared to the single protein but increased predictability compared to a single PROM or QST parameter (Fig. 4A, B). The combination of all three feature dimensions resulted in a framework that views post-incisional outcomes from a molecular, sensory, and psychological perspective, reflecting the complex nature of underlying processes (Fig. 4A, B). On average, an accuracy of 0.76 [0.32–0.97] and 0.74 [0.34–0.96] was achieved for high responders for IncP and HA, respectively. The prognostic predictive models for both outcome measures differed in their composition, while the accuracy of the prediction was comparable.
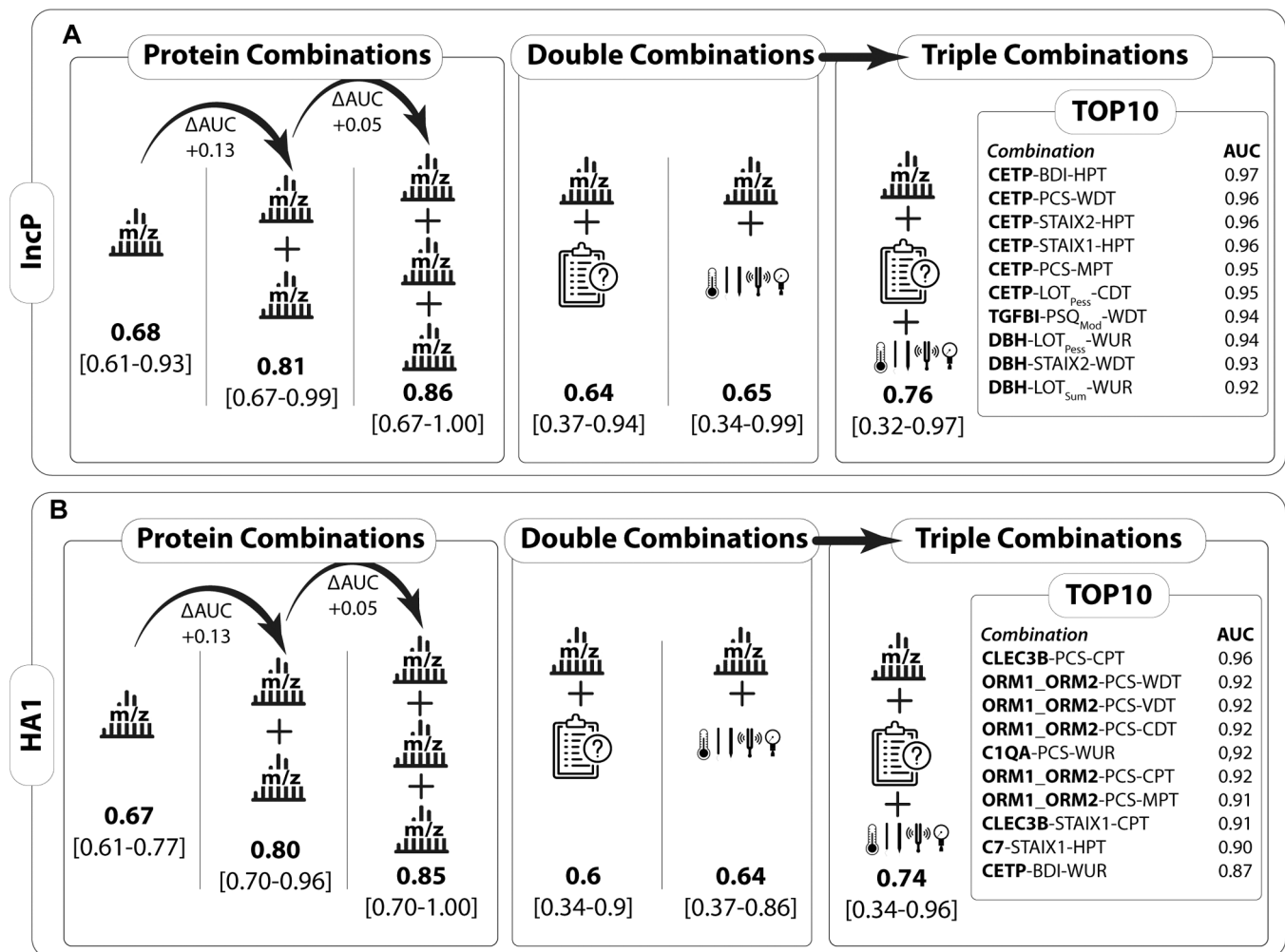
Fig. 4. Improved accuracy in predicting post-incision outcomes using data-driven combinations. (A) For IncP, data-driven prognostic prediction models using multiple QST parameters or PROMs resulted in a slight increase in predictive accuracy compared to using a single parameter. QST and PROMs combined did not improve accuracy. Multiple proteins improved IncP model accuracy. Integrating proteins with QST and PROMs proved beneficial. Molecular, sensory, and psychological factors formed a comprehensive predictive framework for IncP, despite similar accuracy across models. (B) For the outcome HA, a similar pattern was observed. Combining QST, PROMs, or both offered no significant model improvement. Improved HA prediction resulted from multiple proteins. Results improve with protein-QST-PROM combinations. Integrating all three feature dimensions provided a multifaceted perspective, though HA prediction accuracy remained comparable. Prediction accuracy was similar across top 10 combinations, emphasizing the need for multi-dimensional analysis of post-incision responses. Abbreviations: CETP=Cholesteryl Ester Transfer Protein, CGT=Cystathionine Gamma-Lyase, C1QA=Complement C1qa, CLEC3B=C-Type Lectin Domain Family 3 Member B, DBH=Dopamine Beta-Hydroxylase, HPT=Heat Pain Threshold, 5, ORM1 =Orosomucoid 1, ORM2 =Orosomucoid 2, PCP=Pyridoxal Phosphate, TGFBI=-Transforming Growth Factor Beta Induced, BDI=Beck Depression Inventory, PCS=Pain Catastrophizing Scale, PSQ-MOD= Pain Sensitivity Questionnaire-Moderate, STAI x1 = State-Trait Anxiety Inventory Form X1, STAI x2 = State-Trait Anxiety Inventory Form X2, CDT=Cold Detection Threshold, CPT=Cold Pain Threshold, MPT=Mechanical Pain Threshold, VDT=Vibration Detection Threshold, WDT=Warmth Detection Threshold, WUR=Wind-Up Ratio. Mean ROCAUC [min-max range].

3.4. Molecular insights into peripheral and central sensitization post-incision: prognostic prediction models and network-based drug repositioning

Next, we aimed at exploring molecular signatures and pathways within pre-incisional proteome signatures to identify mechanisms underlying low and high responder phenotypes in outcome measures (IncP and HA). We focused on those proteins with prognostic value based on our prior ROC analysis (AUC >0.6 and <-0.6). Comparing low (Fig. 5A) and high (Fig. 5B) responder categories for both outcome measures, we observed distinct and overlapping protein signatures. Term-term-interaction (TTI) network analysis was performed for IncP (Fig. 5C) and HA (Fig. 5D), uncovering terms that were enriched in high responders for both outcomes measures, highlighting clusters related to the innate immune and complement system. The identification of pre-incisional proteins in the cascades of the complement system in high

responders for both outcomes could potentially reflect a pre-incisional low-grade inflammatory condition

We then employed network-based drug repositioning offered by the species- and tissue-specific drug signature online platform *PharmOmics*, which leverages existing therapeutic drugs to modulate disease-associated signaling networks (https://mergeomics.research.idre.ucla.edu; [50]). Network drug repositioning was conducted based on high responder proteome signatures (Supplementary Table 2). Upon filtering the results relevant for the hemopoietic and immune system, we obtained 29 significant hits for high responders (Top15 listed in Table 3, Supplementary Table 2). Remarkably, "antidiabetic" drugs, specifically, the Peroxisome proliferator-activated receptor gamma (PPARγ) agonists, Pioglitazone and Rosiglitazone, were associated with proteome signatures in high responders, while Pioglitazone was associated in IncP (Fig. 5E), and Rosiglitazone in HA (Fig. 5F). The protein-protein-interaction (PPI)-network analysis showed the presence
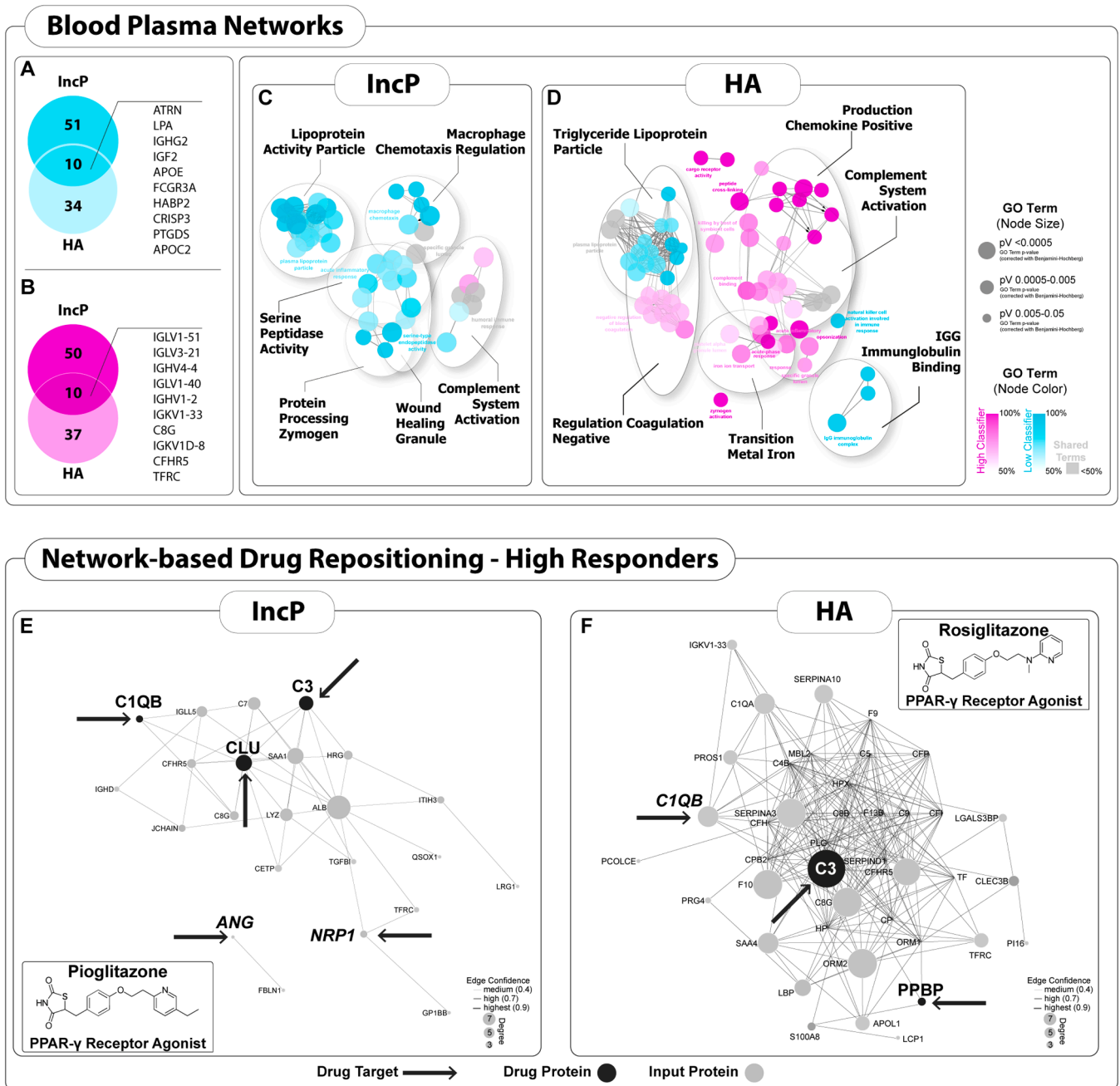
Fig. 5. Molecular mechanistic understanding and network-based drug repositioning analysis for pre-incisional biomarker signatures. (A) Pre-incisional protein patterns for low responders. A total of 51 unique proteins were identified for IncP and 34 for HA in low responders, with an overlap of 10. (B) Pre-incisional protein patterns for high responders. A total of 50 unique proteins were identified for IncP and 37 for HA in high responders, with an overlap of 10. (C) Enriched term-term interaction (TTI)-network analysis for IncP, highlighting terms only present in high responders, particularly clusters related to the innate immune system and the complement system via the classical and alternative pathways. (D) TTI-network analysis for HA, emphasizing terms exclusively present in high responders, with a focus on the complement system and innate immune response pathways. The data reveals significantly enriched GO terms, as indicated by P-values below 0.05, after applying the Benjamini-Hochberg correction. These terms are observed within a functionally grouped network, which accurately represents their interconnected relationships. Each node corresponds to a molecular function or process. Node colors are associated with phenotyping (high responder in magenta shades; low-responder in cyan shades). Gray shades reflect unspecific terms which belong to both responder types. (E) Protein-protein-interaction (PPI) network drug repositioning results for IncP, showing the presence of the PPARγ agonist Pioglitazone and its associated drug protein proteins (CLU, C3, C1QB), including ANG and NRP1 as input proteins. (F) PPI-network drug repositioning results for HA, indicating the PPARγ agonist Rosiglitazone and its associated drug proteins (C3, PPBP), with C1QB also identified as an input protein.

of five drug proteins (C1QB, C3, CLU, ANG, NRP1) for Pioglitazone in IncP and three proteins as targets (C1QB, C3, PPBP) for Rosiglitazone in HA.

Recently, DuBreuil et al. showed that human serum could excite dorsal root ganglion (DRG) neurons *in vitro* [55]. As DRG are exposed to

proteins circulating in the blood, we looked for potential interactions between the blood proteins defining the pre-incisional protein signature of high responders with receptors expressed in human DRG (see Supplementary Table 3 for all potential ligand-receptor interactions) by using the Sensoryomics Interactome resource from the Center for

Table 3

Network-based drug repositioning with PharmOmics: detailed Z-Scores, rankings, and p-values.

Drug	Tissue	Z_score	Rank	P-value
Atorvastatin	hematopoietic system	−3.59	0.9968	0.000
Immunosuppressant	immune system	−2.55	0.9959	0.005
Alkylating agent	immune system	−2.55	0.9951	0.005
Rosiglitazone	hematopoietic system	−2.51	0.9951	0.006
Infliximab	hematopoietic system	−2.50	0.9943	0.006
Cyclophosphamide	immune system	−2.48	0.9935	0.007
Anti-TNF-alpha antibody	hematopoietic system	−2.47	0.9927	0.007
Rosuvastatin	hematopoietic system	−2.46	0.9967	0.007
Antimetabolite	immune system	−2.39	0.9959	0.009
Arsenic trioxide	hematopoietic system	−2.31	0.9783	0.010
Fludarabine	immune system	−2.27	0.9934	0.012
COX inhibitor	hematopoietic system	−2.27	0.9759	0.012
Antidiabetic	hematopoietic system	−2.24	0.9918	0.013
PPARγ gamma agonist	hematopoietic system	−2.21	0.9910	0.013
Etoposide	immune system	−2.17	0.9780	0.015

Advanced Pain Studies (https://sensoryomics.shinyapps.io/Interactome/). Several blood proteins of the PPI-network displayed in Fig. 5 E, F were found to be reported as potential ligands of receptors expressed in human nociceptors (e.g., SAA1, C1QB, ANG, C5, QSOX1, C1QA, ALB). Interestingly, some (e.g., C1QB, ANG) of these may be directly targeted by aforementioned antidiabetics (suggested by the drug repositioning approach, Fig. 5 E, F) or indirectly targeted within the PPI-network (e.g., SAA1, C5, QSOX1, C1QA, ALB, HRG, LYZ).

4. Discussion

Although guidelines and procedure-specific evidence-based recommendations for postsurgical pain management exist [56,57], a high number of patients still experience severe pain after surgery, which impacts not only their quality of recovery but also long-term outcome, including CPSP [4,58]. Because certain patients are more susceptible to experiencing acute pain and developing CPSP, timely identification of high-risk patients for severe postsurgical pain and CPSP is imperative, but still poses a significant challenge. While several models for the prediction of CPSP have been developed, most exhibit significant limitations, e.g. a high risk of bias that affects their reliability [11]. Another current challenge is the incomplete understanding of the underlying mechanisms relevant for developing CPSP, e.g. by addressing comprehensively the bio-psycho-social aspect of chronic pain in such models [11,14,59]. Most prediction models rely on demographics (age,sex and/or gender), or preoperative pain characteristics, while incorporating molecular markers or psychological factors (or best both) remains limited [11,14]. In fact, no previous study has employed unbiased blood proteome profiling, neither in an experimental or clinical setting, and combining it with other factors to integrate proteins into prognostic prediction models. To date, only models incorporating hypothesis-based approaches with a specific protein panel have been established and documented for CPSP [59–61].

We show here that our multi-modal framework, including unbiased proteome analysis effectively enabled the identification of high and low responders for relevant outcome measures related to pain after surgery. Several factors qualified as adequate predictors of high responders, including psychological characteristics and psycho-physical testing, and combining factors, improved prediction value. Nevertheless, the overall predictive accuracy of models include these features remains moderate [11,62,63]. However, including findings from our unbiased blood plasma proteome analysis enhanced prediction accuracy. We acknowledge the experimental design and small volunteer cohort. Still, our study, designed as a proof-of-concept study, highlights for the first time the promising role of proteins, identified with an unbiased approach, in predicting with high accuracy severe acute and chronic postsurgical pain phenotypes. Future prospective trials, e.g. in large patient cohorts,

should confirm our results and determine proteomic profiles predicting pain phenotypes including CPSP.

A synergistic effect on predictive capability may be achieved by incorporating clinical parameters with proteome analysis. By integrating an unbiased proteomic approach with advanced sensory testing and PROMs, we achieved an even more accurate predictive capability. These data postulate that integrating plasma proteome signatures acquired prior to surgery may facilitate the prediction of CPSP in an integrative approach [59]. Interestingly, the multi-feature prognostic predictive models were composed differently for each outcome measure, yet the accuracy of the prediction remained comparable, emphasizing the distinct nature of post-incisional outcomes. These results support the bio-psycho-social complex nature of (postoperative) chronic pain. Certainly, translational approaches in larger cohorts and validation of our results in patients are required before these results can be transferred to clinical practice. The success of introducing such pipelines into clinical routine also needs to consider time and economic factors while providing high-throughput and standardized features [64]. This involves developing streamlined protocols that balance patient/provider burden with model predictive power. Practicability and scalability of prognostic predictive models in clinical settings can be improved through efficient and cost-effective methods. However, if validated for clinical use, analysis of blood plasma by using for example ELISAs exhibits several advantages for clinical proteome profiling given that it is easy-to-be-collected (following standardized procedures) and small volumes suffice for downstream molecular analysis [15,16,47].

Integrating proteomics in prediction models may not only improve pre-surgical diagnostic prediction of those patients with a high risk of severe acute pain and CPSP after surgery. It might additionally enable the development of (new) preventive treatment approaches, including the identification of new drug targets. Therefore, by analyzing pre-incisional TTI-networks, we sought to understand the molecular mechanisms of high versus low responders regarding both outcome measures. Most intriguingly , proteomic features of responder types pointed towards the involvement of the innate immune system in high responders for both outcome measures. These findings are in accordance with recent studies in patients with neuropathic pain post-surgery [65]. The results suggest that high responders display a low-grade inflammatory status. Low-grade inflammation refers to a mild state of inflammation representing chronic, yet subtle activation of the immune system [66, 67]. Unlike acute inflammation, chronic low-grade inflammation is typically asymptomatic [66]. Proteins identified by us as being relevant for prediction of high responders, such as LRG1, TFRC, LYZ, or SAA1, play critical roles in chronic low-grade inflammation. The involvement of these proteins lies in their ability to promote immune cell migration, enhance inflammatory signaling pathways, and modulate tissue remodeling, all of which are critical factors in the maintenance of persistent inflammation. For example, LRG1 is known to enhance immune cell infiltration and activation, contributing to prolonged inflammatory responses [68]. SAA1 acts as an acute-phase reactant and chemokine, accelerating response to inflammation and perpetuating immune activation in chronic conditions [69] by interacting with formyl peptide like receptors 1 and 2 (FPLR1 and FPLR2) in human monocytes and neutrophils. This protein facilitates chemotaxis and augments calcium flux, resulting in the activation of mitogen-activated protein kinases (MAPKs) and nuclear factor kappa B (NFκB) pathways, subsequently leading to the secretion of tumor necrosis factor alpha (TNFα), interleukin-8 (IL-8), and monocyte chemotactic protein-1 (MCP-1) [70,71]. The occurrence of low-grade inflammation can enhance the release of cytokines and other signaling molecules, thereby sensitizing pain receptors. Chronic stress, an unhealthy diet, obesity, lack of exercise, smoking, chronic infections, and autoimmune disorders can all contribute to low-grade inflammation [72,73]. Ongoing interactions between the immune and nervous system can exacerbate and sustain nociceptive signals and be accompanied by the release of pro-inflammatory cytokines and other mediators. In the future, the

proteome signature could not only enable us to identify those patients with low-grade inflammation and at risk for negative pain outcomes, but it might also facilitate their prevention.

Intriguingly, our results suggest that targeting the low-grade inflammation in patients at risk may curb postoperative complications in future clinical scenarios. Along these lines, we employed a computational network-based approach to repurpose available drugs. Drug repositioning identifies new uses for existing drugs, accelerating development and offering cost-effective treatments. Using this approach, we identified PPARγ agonists such as Rosiglitazone and Pioglitazone as potential modulators of low-grade inflammation [74] associated with identified protein networks. Indeed, local Rosiglitazone administration reduced hypersensitivity in a mouse incision pain model, dampening post-incisional inflammation and hypersensitivity by modulating macrophage polarity [75]. Also, the PPARγ agonist Pioglitazone has been reported in several preclinical studies to exert an anti-hypersensitivity effect in a variety of pain models ranging from inflammatory, post-incisional, to neuropathic pain [76–79]. Considering evidence in preclinical studies for PPARγ agonists in attenuating pain, further studies to investigate the underlying mechanisms and the site of action are warranted [77]. Even though underlying mechanisms may be complex, our data may offer an intriguing hypothesis: We observed that several identified blood proteins could serve as ligands for nociceptors in DRG (e.g., SAA1, C5, QSOX1, C1QA, ALB, HRG, LYZ;Supplementary Table 3). Thus, targeting these blood proteins with repositioned drugs may directly or indirectly - via effects on protein networks - modulate DRG physiology and function.

While a clear advantage of drug repurposing is that the safety profile characteristics of the compound in question are already known, the effective dosage and time point of intervention would need additional investigations. Along these lines, network-based medicine aims to harness potential synergistic drug combinations that target multiple signaling pathways within disease-associated networks [80–82]. For example, in the context of our results, it is conceivable that anti-inflammatory drugs, immunomodulators, and metabolic modulators may be combined at lower doses to synergistically target inflammatory pathways and, in parallel, reduce potential side effects. Certainly, large study cohorts are required to predict effects (both therapeutic and adverse effects) and drug-drug interactions when combining multiple drugs and their interactions.

While the development of novel analgesics has historically been challenging, with ample setbacks, drug repurposing and network medicine may offer a valuable alternative approach for future pain management.

5. Limitations

The development of prognostic prediction models is associated with several difficulties that must be addressed to ensure their robustness [11]. In this proof-of-concept study, we employed a tightly controlled experimental model for post-surgical pain, using a small, homogeneous sample of young male participants. This design aimed to minimize degrees of freedom, reduce the overestimation of multi-feature models, but limits the external validity and generalizability to broader populations. Furthermore, model over-fitting is a concern due to a large number of variables, especially with the unbiased protein list. To improve validity, models should be tested on independent and larger cohorts with varied sex and/or gender and age [11].

Our efforts to enhance model accuracy by combining molecular data with psychological or psycho-physical factors did yield slightly better performance compared to using individual psychological or psycho-physical features alone. This may be due to the complexity and variability in how different data types interact. Proteomic data is (semi-) quantitative and high-dimensional, while psychological and psycho-physical data is more qualitative and subjective. Integrating these disparate data types can introduce noise and complicate modeling.

Increasing the number of variables without adding predictive power may lead to model overfitting, where models perform well on training data but poorly on new data [83]. Future studies should focus on (i) increasing sample size, (ii) using independent datasets for validation, and (iii) performing longitudinal monitoring. Adopting this stepwise, iterative process will help refine the methods established here, ultimately advancing toward clinically meaningful predictions of chronic post-surgical pain in diverse patient populations.

6. Conclusion

This study integrated unbiased blood plasma proteomics, psychophysical, and psychological profiles to develop data-driven prognostic prediction models for distinct pain-related outcome measures following an experimental incision. These outcomes include pain intensity (IncP) and mechanical hyperalgesia (HA), which serves as a proxy of central sensitization [84,85] and as a predictor of chronic pain in patients after surgery [40,41,86]. Applying data-driven multi-feature combinations resulted in an enhanced accuracy of prognostic prediction models, effectively capturing multiple aspects relevant for pain, with proteins being most predictive. Protein network analysis revealed a pre-incisional low-grade inflammatory response in high responders, potentially contributing to heightened IncP and pronounced HA. Network-based drug repositioning highlighted PPARγ agonists as possible treatment options for low-grade inflammation in high responders. Our integrative approach, which combines multi-level data-driven prognostic prediction models, proteomics and network-based drug repositioning, is highly valuable for future clinical studies. It may be used for large clinical cohorts to better understand and predict both acute and chronic postsurgical pain (CPSP), and to develop new, target-specific drugs and drug combinations.

Clinical trial number and registry URL

DRKS00016641 (https://drks.de/search/de/trial/DRKS00016641), Prof. Dr. med. Esther Pogatzki-Zahn, Registration: 06/02/2019

CRediT authorship contribution statement

Esther Miriam Pogatzki-Zahn: Writing – review & editing, Writing – original draft, Visualization, Validation, Supervision, Resources, Project administration, Methodology, Funding acquisition, Conceptualization. **Christin Kappert:** Writing – original draft, Investigation, Formal analysis. **Bruno Pradier:** Writing – review & editing, Methodology, Investigation, Formal analysis, Data curation. **Daniel Segelcke:** Writing – review & editing, Writing – original draft, Visualization, Methodology, Investigation, Data curation, Conceptualization. **Julia Regina Sondermann:** Writing – original draft, Methodology, Investigation, Data curation, Formal analysis. **Jan Vollert:** Writing – original draft, Investigation, Formal analysis, Data curation. **Peter Konrad Zahn:** Writing – review & editing, Supervision, Resources, Conceptualization. **Dennis Görlich:** Investigation, Formal analysis. **Manfred Fobker:** Writing – review & editing, Investigation. **Manuela Schmidt:** Writing – review & editing, Writing – original draft, Visualization, Supervision, Resources, Funding acquisition, Conceptualization.

Abbreviation (description)

AUC	Area Under the Curve — A statistical measure used in this context to evaluate pain intensity over time.
BDI	Beck Depression Inventory — A self-report questionnaire used to assess the severity of depression.
CDT	Cold Detection Threshold — The point at which cold is detected as a stimulus.
CPT	Cold Pain Threshold — The lowest temperature at which cold becomes painful.
CPSP	Chronic Post-Surgical Pain — Pain that persists after a surgical procedure for at least three months, beyond the healing process.
DIA	Data-Independent Acquisition — A mass spectrometry technique used to quantify proteins by acquiring data from all peptides in a sample, regardless of their abundance.
HA	Hyperalgesic Area — An area around the incision site that exhibits increased sensitivity to mechanical stimuli, used as a proxy for central sensitization.
HPT	Heat Pain Threshold — The lowest temperature at which heat becomes painful.
ICD	International Classification of Diseases — A globally used diagnostic tool for epidemiology, health management, and clinical purposes.
IncP	Incisional Pain — Pain intensity measured immediately after an incision.
LOOCV	Leave-One-Out Cross-Validation — A statistical method used to validate predictive models by testing one data point at a time.
MDT	Mechanical Detection Threshold — The minimum stimulus required to produce a mechanical sensation.
MPS	Mechanical Pain Sensitivity — The sensitivity to pain caused by mechanical stimuli.
MSA	Mass Spec Analysis — Refers to the process of analyzing mass spectrometry data to identify proteins.
MS	Mass Spectrometry — A technology used to identify and quantify proteins and other biomolecules by measuring their mass-to-charge ratio.
PCS	Pain Catastrophizing Scale — A questionnaire to assess the degree to which a person catastrophizes their perception of pain.
PPARγ	Peroxisome Proliferator-Activated Receptor Gamma — A type of nuclear receptor that regulates gene expression and is associated with metabolism and inflammation.
PPI	Protein-Protein Interaction — The physical contacts between two or more proteins within a cell.
PSQ	Pain Sensitivity Questionnaire — A measure used to evaluate an individual's sensitivity to pain.
QST	Quantitative Sensory Testing — A method to assess sensory nerve function by applying stimuli such as temperature or pressure to the skin.
STAI	State-Trait Anxiety Inventory — A tool used to measure both the transient state and the long-term trait of anxiety in individuals.
VDT	Vibration Detection Threshold — The lowest intensity of vibration that can be felt by the subject.
WDT	Warm Detection Threshold — The point at which warmth is detected as a stimulus.
WUR	Wind-Up Ratio — A measure of increased pain sensitivity caused by repeated stimulation.

Declaration of Competing Interest

Acknowledgments

Appendix A. Supporting information

Supplementary data associated with this article can be found in the online version at doi:10.1016/j.phrs.2025.107580.

References

[1] T.G. Weiser, A.B. Haynes, G. Molina, S.R. Lipsitz, M.M. Esquivel, T. Uribe-Leitz, R. Fu, T. Azad, T.E. Chao, W.R. Berry, A.A. Gawande, Size and distribution of the global volume of surgery in 2012, Bull. World Health Organ. 94 (2016) 201–209F, https://doi.org/10.2471/BLT.15.159293.

[2] R.L.M. van Boekel, M.C. Warlé, R.G.C. Nielen, K.C.P. Vissers, R. van der Sande, E. M. Bronkhorst, J.G.C. Lerou, M.A.H. Steegers, Relationship between postoperative pain and overall 30-day complications in a broad surgical population: an observational study, Ann. Surg. (2017), https://doi.org/10.1097/SLA.0000000000002583.

[3] T.J. Gan, A.S. Habib, T.E. Miller, W. White, J.L. Apfelbaum, Incidence, patient satisfaction, and perceptions of post-surgical pain: results from a US national survey, Curr. Med. Res. Opin. 30 (2014) 149–160, https://doi.org/10.1185/03007995.2013.860019.

[4] P. Glare, K.R. Aubrey, P.S. Myles, Transition from acute to chronic pain after surgery, Lancet 393 (2019) 1537–1546, https://doi.org/10.1016/S0140-6736(19)30352-6.

[5] E.C. Sun, B.D. Darnall, L.C. Baker, S. Mackey, Incidence of and risk factors for chronic opioid use among opioid-naïve patients in the postoperative period, JAMA Intern. Med. 176 (2016) 1286–1293, https://doi.org/10.1001/jamainternmed.2016.3298.

[6] S.A. Schug, P. Lavand'homme, A. Barke, B. Korwisi, W. Rief, R.-D. Treede, The IASP classification of chronic pain for ICD-11: chronic postsurgical or posttraumatic pain, Pain 160 (2019) 45–52, https://doi.org/10.1097/j.pain.0000000000001413.

[7] D. Fletcher, U.M. Stamer, E. Pogatzki-Zahn, R. Zaslansky, N.V. Tanase, C. Perruchoud, P. Kranke, M. Komann, T. Lehman, W. Meissner, Chronic postsurgical pain in Europe: an observational study, Eur. J. Anaesthesiol. 32 (2015) 725–734, https://doi.org/10.1097/EJA.0000000000000319.

[8] M.E. Carley, L.E. Chaparro, M. Choinière, H. Kehlet, R.A. Moore, E. van den Kerkhof, I. Gilron, Pharmacotherapy for the prevention of chronic pain after surgery in adults: an updated systematic review and meta-analysis, Anesthesiology 135 (2021) 304–325, https://doi.org/10.1097/ALN.0000000000003837.

[9] D.C. Rosenberger, E.M. Pogatzki-Zahn, Chronic post-surgical pain – update on incidence, risk factors and preventive treatment options, BJA Educ. 22 (2022) 190–196, https://doi.org/10.1016/j.bjae.2021.11.008.

[10] D.C. Rosenberger, D. Segelcke, E.M. Pogatzki-Zahn, Mechanisms inherent in acute-to-chronic pain after surgery - risk, diagnostic, predictive, and prognostic factors, Curr. Opin. Support. Palliat. Care (2023), https://doi.org/10.1097/SPC.0000000000000673.

[11] N. Papadomanolakis-Pakis, P. Uhrbrand, S. Haroutounian, L. Nikolajsen, Prognostic prediction models for chronic postsurgical pain in adults: a systematic review, Pain 162 (2021) 2644–2657, https://doi.org/10.1097/j.pain.0000000000002261.

[12] A. Montes, G. Roca, J. Cantillo, S. Sabate, Presurgical risk model for chronic postsurgical pain based on 6 clinical predictors: a prospective external validation, Pain 161 (2020) 2611–2618, https://doi.org/10.1097/j.pain.0000000000001945.

[13] A. Montes, G. Roca, S. Sabate, J.I. Lao, A. Navarro, J. Cantillo, J. Canet, Genetic and clinical factors associated with chronic postsurgical pain after hernia repair, hysterectomy, and thoracotomy, Anesthesiology 122 (2015) 1123–1141, https://doi.org/10.1097/ALN.0000000000000611.

[14] D. Segelcke, D. Rosenberger, E.M. Pogatzki-Zahn, Prognostic models for chronic postsurgical pain-current developments, trends, and challenges, Curr. Opin. Anaesthesiol. (2023), https://doi.org/10.1097/ACO.0000000000001299.

[15] P.E. Geyer, L.M. Holdt, D. Teupser, M. Mann, Revisiting biomarker discovery by plasma proteomics, Mol. Syst. Biol. 13 (2017) 942, https://doi.org/10.15252/msb.20156297.

[16] P.E. Geyer, N.A. Kulak, G. Pichler, L.M. Holdt, D. Teupser, M. Mann, Plasma proteome profiling to assess human health and disease, Cell Syst. 2 (2016) 185–195, https://doi.org/10.1016/j.cels.2016.02.015.

[17] Y. Guo, J. You, Y. Zhang, W.-S. Liu, Y.-Y. Huang, Y.-R. Zhang, W. Zhang, Q. Dong, J.-F. Feng, W. Cheng, J.-T. Yu, Plasma proteomic profiles predict future dementia in healthy adults, Nat. Aging (2024), https://doi.org/10.1038/s43587-023-00565-0.

[18] U. Azmat, K. Porter, L. Senter, M.D. Ringel, F. Nabhan, Thyroglobulin liquid chromatography-tandem mass spectrometry has a low sensitivity for detecting structural disease in patients with antithyroglobulin antibodies, Thyroid 27 (2017) 74–80, https://doi.org/10.1089/thy.2016.0210.

[19] C. Spencer, J. LoPresti, S. Fatemi, How sensitive (second-generation) thyroglobulin measurement is changing paradigms for monitoring patients with differentiated thyroid cancer, in the absence or presence of thyroglobulin autoantibodies, Curr. Opin. Endocrinol. Diabetes Obes. 21 (2014) 394–404, https://doi.org/10.1097/MED.0000000000000092.

[20] M. Ho, G. Bianchi, K.C. Anderson, Proteomics-inspired precision medicine for treating and understanding multiple myeloma, Expert Rev. Precis. Med. Drug Dev. 5 (2020) 67–85, https://doi.org/10.1080/23808993.2020.1732205.

[21] T. Rezk, J.A. Gilbertson, P.P. Mangione, D. Rowczenio, N.B. Rendell, D. Canetti, H. J. Lachmann, A.D. Wechalekar, P. Bass, P.N. Hawkins, V. Bellotti, G.W. Taylor, J. D. Gillmore, The complementary role of histology and proteomics for diagnosis and typing of systemic amyloidosis, J. Pathol. Clin. Res. 5 (2019) 145–153, https://doi.org/10.1002/cjp2.126.

[22] C. Brede, B. Hop, K. Jørgensen, Ø. Skadberg, Measurement of glycated albumin in serum and plasma by LC-MS/MS, Scand. J. Clin. Lab. Invest. 76 (2016) 195–201, https://doi.org/10.3109/00365513.2015.1129671.

[23] C. Bystrom, S. Sheng, K. Zhang, M. Caulfield, N.J. Clarke, R. Reitz, Clinical utility of insulin-like growth factor 1 and 2; determination by high resolution mass spectrometry, PLoS ONE 7 (2012) e43457, https://doi.org/10.1371/journal.pone.0043457.

[24] Y. Gui, Y. Lu, S. Li, M. Zhang, X. Duan, C.C. Liu, J. Jia, G. Liu, Direct analysis in real time-mass spectrometry for rapid quantification of five anti-arrhythmic drugs in human serum: application to therapeutic drug monitoring, Sci. Rep. 10 (2020) 15550, https://doi.org/10.1038/s41598-020-72490-w.

[25] E.M. Pogatzki-Zahn, C. Wagner, A. Meinhardt-Renner, M. Burgmer, C. Beste, P. K. Zahn, B. Pfleiderer, Coding of incisional pain in humans: a functional magnetic resonance imaging study in human volunteers, Anesthesiology 112 (2010) 406–417, https://doi.org/10.1097/ALN.0b013e3181ca4c82.

[26] E.M. Pogatzki-Zahn, C. Drescher, J.S. Englbrecht, T. Klein, W. Magerl, P.K. Zahn, Progesterone relates to enhanced incisional acute pain and pinprick hyperalgesia in the luteal phase of female volunteers, Pain 160 (2019) 1781–1793, https://doi.org/10.1097/j.pain.0000000000001561.

[27] D. Segelcke, M. van der Burgt, C. Kappert, D. Schmidt Garcia, J.R. Sondermann, S. Bigalke, B. Pradier, D. Gomez-Varela, P.K. Zahn, M. Schmidt, E.M. Pogatzki-Zahn, Phenotype- and species-specific skin proteomic signatures for incision-induced pain in humans and mice, Br. J. Anaesth. 130 (2023) 331–342, https://doi.org/10.1016/j.bja.2022.10.040.

[28] R. Rolke, R. Baron, C. Maier, T.R. Tölle, R.-D. Treede, A. Beyer, A. Binder, N. Birbaumer, F. Birklein, I.C. Bötefür, S. Braune, H. Flor, V. Huge, R. Klug, G. B. Landwehrmeyer, W. Magerl, C. Maihöfner, C. Rolko, C. Schaub, A. Scherens, T. Sprenger, M. Valet, B. Wasserka, Quantitative sensory testing in the German Research Network on Neuropathic Pain (DFNS): standardized protocol and reference values, Pain 123 (2006) 231–243, https://doi.org/10.1016/j.pain.2006.01.041.

[29] D. Yarnitsky, E. Sprecher, R. Zaslansky, J.A. Hemli, Heat pain thresholds: normative data and repeatability, Pain 60 (1995) 329–332.

[30] I. Fimer, T. Klein, W. Magerl, R.-D. Treede, P.K. Zahn, E.M. Pogatzki-Zahn, Modality-specific somatosensory changes in a human surrogate model of postoperative pain, Anesthesiology 115 (2011) 387–397, https://doi.org/10.1097/ALN.0b013e318219509e.

[31] R. Ruscheweyh, M. Marziniak, F. Stumpenhorst, J. Reinholz, S. Knecht, Pain sensitivity can be assessed by self-rating: Development and validation of the Pain Sensitivity Questionnaire, Pain 146 (2009) 65–74, https://doi.org/10.1016/j.pain.2009.06.020.

[32] A.T. BECK, C.H. WARD, M. MENDELSON, J. MOCK, J. ERBAUGH, An inventory for measuring depression, Arch. Gen. Psychiatry 4 (1961) 561–571.

[33] R. Ruscheweyh, B. Verneuer, K. Dany, M. Marziniak, A. Wolowski, R. Colak-Ekici, T.L. Schulte, V. Bullmann, S. Grewe, I. Gralow, S. Evers, S. Knecht, Validation of the pain sensitivity questionnaire in chronic pain patients, Pain 153 (2012) 1210–1218, https://doi.org/10.1016/j.pain.2012.02.025.

[34] C.D. Spielberger, Manual for the State -Trait Anxiety Inventory (STAI), Consulting Psychologist Press, Palo Alto, CA, 1983.

[35] M.J.L. Sullivan, S.R. Bishop, J. Pivik, The pain catastrophizing scale: development and validation, Psychol. Assess. 7 (1995) 524–532, https://doi.org/10.1037/1040-3590.7.4.524.

[36] M. Kawamata, H. Watanabe, K. Nishikawa, T. Takahashi, Y. Kozuka, T. Kawamata, K. Omote, A. Namiki, Different mechanisms of development and maintenance of experimental incision-induced hyperalgesia in human skin, Anesthesiology 97 (2002) 550–559.

[37] E.M. Pogatzki-Zahn, H. Liedgens, L. Hummelshoj, W. Meissner, C. Weinmann, R.-D. Treede, K. Vincent, P. Zahn, U. Kaiser, Developing consensus on core outcome domains for assessing effectiveness in perioperative pain management: results of the PROMPT/IMI-PainCare Delphi Meeting, Pain 162 (2021) 2717–2736, https://doi.org/10.1097/j.pain.0000000000002254.

[38] J.C. Eisenach, Preventing chronic pain after surgery: who, how, and when? Reg. Anesth. Pain. Med. 31 (2006) 1–3, https://doi.org/10.1016/j.rapm.2005.11.008.

[39] M. de Kock, P. Lavand'homme, H. Waterloos, 'Balanced analgesia' in the perioperative period: is there a place for ketamine? Pain 92 (2001) 373–380, https://doi.org/10.1016/S0304-3959(01)00278-0.

[40] V. Martinez, S.Ben Ammar, T. Judet, D. Bouhassira, M. Chauvin, D. Fletcher, Risk factors predictive of chronic postsurgical neuropathic pain: the value of the iliac crest bone harvest model, Pain 153 (2012) 1478–1483, https://doi.org/10.1016/j.pain.2012.04.004.

[41] P. Lavand'homme, M. de Kock, H. Waterloos, Intraoperative epidural analgesia combined with ketamine provides effective preventive analgesia in patients undergoing major digestive surgery, Anesthesiology 103 (2005) 813–820, https://doi.org/10.1097/00000542-200510000-00020.

[42] T. Masuda, M. Tomita, Y. Ishihama, Phase transfer surfactant-aided trypsin digestion for membrane proteome analysis, J. Proteome Res. 7 (2008) 731–740, https://doi.org/10.1021/pr700658q.

[43] C. Escher, L. Reiter, B. MacLean, R. Ossola, F. Herzog, J. Chilton, M.J. MacCoss, O. Rinner, Using iRT, a normalized retention time for more targeted measurement of peptides, Proteomics 12 (2012) 1111–1121, https://doi.org/10.1002/pmic.201100463.

[44] V. Demichev, C.B. Messner, S.I. Vernardis, K.S. Lilley, M. Ralser, DIA-NN: neural networks and interference correction enable deep proteome coverage in high throughput, Nat. Methods 17 (2020) 41–44, https://doi.org/10.1038/s41592-019-0638-x.

[45] J. Cox, M.Y. Hein, C.A. Luber, I. Paron, N. Nagaraj, M. Mann, Accurate proteome-wide label-free quantification by delayed normalization and maximal peptide ratio extraction, termed MaxLFQ, Mol. Cell. Proteom. 13 (2014) 2513–2526, https://doi.org/10.1074/mcp.M113.031591.

[46] Y. Perez-Riverol, A. Csordas, J. Bai, M. Bernal-Llinares, S. Hewapathirana, D. J. Kundu, A. Inuganti, J. Griss, G. Mayer, M. Eisenacher, E. Pérez, J. Uszkoreit, J. Pfeuffer, T. Sachsenberg, S. Yilmaz, S. Tiwary, J. Cox, E. Audain, M. Walzer, A. F. Jarnuczak, T. Ternent, A. Brazma, J.A. Vizcaíno, The PRIDE database and related tools and resources in 2019: improving support for quantification data, Nucleic Acids Res. 47 (2019) D442–D450, https://doi.org/10.1093/nar/gky1106.

[47] P.E. Geyer, E. Voytik, P.V. Treit, S. Doll, A. Kleinhempel, L. Niu, J.B. Müller, M.-L. Buchholtz, J.M. Bader, D. Teupser, L.M. Holdt, M. Mann, Plasma Proteome Profiling to detect and avoid sample-related biases in biomarker studies, EMBO Mol. Med. 11 (2019) e10427, https://doi.org/10.15252/emmm.201910427.

[48] A. Franceschini, D. Szklarczyk, S. Frankild, M. Kuhn, M. Simonovic, A. Roth, J. Lin, P. Minguez, P. Bork, C. von Mering, L.J. Jensen, STRING v9.1: protein-protein interaction networks, with increased coverage and integration, Nucleic Acids Res 41 (2013) D808–D815, https://doi.org/10.1093/nar/gks1094.

[49] P. Shannon, A. Markiel, O. Ozier, N.S. Baliga, J.T. Wang, D. Ramage, N. Amin, B. Schwikowski, T. Ideker, Cytoscape: a software environment for integrated models of biomolecular interaction networks Genome, Research 13 (11) (2003) 2498–2504.

[50] Y.-W. Chen, G. Diamante, J. Ding, T.X. Nghiem, J. Yang, S.-M. Ha, P. Cohn, D. Arneson, M. Blencowe, J. Garcia, N. Zaghari, P. Patel, X. Yang, PharmOmics: A species- and tissue-specific drug signature database and gene-network-based drug repositioning tool, iScience 25 (2022) 104052, https://doi.org/10.1016/j.isci.2022.104052.

[51] A. Wangzhou, C. Paige, S.V. Neerukonda, D.K. Naik, M. Kume, E.T. David, G. Dussor, P.R. Ray, T.J. Price, A ligand-receptor interactome platform for discovery of pain mechanisms and therapeutic targets, Sci. Signal. 14 (2021), https://doi.org/10.1126/scisignal.abe1648.

[52] S.A. Bhuiyan, M. Xu, L. Yang, E. Semizoglou, P. Bhatia, K.I. Pantaleo, I. Tochitsky, A. Jain, B. Erdogan, S. Blair, V. Cat, J.M. Mwirigi, I. Sankaranarayanan, D. Tavares-Ferreira, U. Green, L.A. McIlvried, B.A. Copits, Z. Bertels, J.S. Del Rosario, A. J. Widman, R.A. Slivicki, J. Yi, C.J. Woolf, J.K. Lennerz, J.L. Whited, T.J. Price, R. W. Gereau, R. Renthal, Harmonized cross-species cell atlases of trigeminal and dorsal root ganglia, bioRxiv (2023), https://doi.org/10.1101/2023.07.04.547740.

[53] D. Tavares-Ferreira, S. Shiers, P.R. Ray, A. Wangzhou, V. Jeevakumar, I. Sankaranarayanan, A.M. Cervantes, J.C. Reese, A. Chamessian, B.A. Copits, P. M. Dougherty, R.W. Gereau, M.D. Burton, G. Dussor, T.J. Price, Spatial transcriptomics of dorsal root ganglia identifies molecular signatures of human nociceptors, Sci. Transl. Med. 14 (2022) eabj8186, https://doi.org/10.1126/scitranslmed.abj8186.

[54] I. Ferrari, S. Mazzara, S. Abrignani, R. Grifantini, M. Bombaci, R.L. Rossi, Combinatorial selection of biomarkers to optimize gene signatures in diagnostics and single cell applications, 2022.

[55] D.M. DuBreuil, B.M. Chiang, K. Zhu, X. Lai, P. Flynn, Y. Sapir, B.J. Wainger, A high-content platform for physiological profiling and unbiased classification of individual neurons, Cell Rep. Methods 1 (2021), https://doi.org/10.1016/j.crmeth.2021.100004.

[56] C. Bourgeois, L. Oyaert, M. van de Velde, E. Pogatzki-Zahn, S.M. Freys, A.R. Sauter, G.P. Joshi, G. Dewinter, Pain management after laparoscopic cholecystectomy: A systematic review and procedure-specific postoperative pain management (PROSPECT) recommendations, Eur. J. Anaesthesiol. (2024), https://doi.org/10.1097/EJA.0000000000002047.

[57] J.C. Freys, S.M. Bigalke, M. Mertes, D.N. Lobo, E.M. Pogatzki-Zahn, S.M. Freys, Perioperative pain management for appendectomy: A systematic review and

Procedure-specific Postoperative Pain Management recommendations, Eur. J. Anaesthesiol. 41 (2024) 174–187, https://doi.org/10.1097/EJA.0000000000001953.

[58] P. Lavand'homme, Transition from acute to chronic pain after surgery, Pain 158 (1) (2017) S50–S54, https://doi.org/10.1097/j.pain.0000000000000809.

[59] E.M. Pogatzki-Zahn, D. Segelcke, Searching for the rainbow: biomarkers relevant for chronic postsurgical pain, Pain 165 (2024) 247–249, https://doi.org/10.1097/j.pain.0000000000003043.

[60] R. Giordano, K.K. Petersen, H.H. Andersen, O. Simonsen, L. Arendt-Nielsen, Serum inflammatory markers in patients with knee osteoarthritis: a proteomic approach, Clin. J. Pain. 36 (2020) 229–237, https://doi.org/10.1097/AJP.0000000000000804.

[61] Giordano R., Ghafouri B. Arendt-Nielsen L., Kjær-Staal Petersen K.

[62] F. Wu, J. Liu, L. Zheng, C. Chen, D. Basnet, J. Zhang, C. Shen, X. Feng, Y. Sun, X. Du, J.C. Zheng, J. Liu, Preoperative pain sensitivity and its correlation with postoperative acute and chronic pain: a systematic review and meta-analysis, Br. J. Anaesth. 133 (2024) 591–604, https://doi.org/10.1016/j.bja.2024.05.010.

[63] M. Braun, C. Bello, T. Riva, C. Hönemann, D. Doll, R.D. Urman, M.M. Luedi, Quantitative sensory testing to predict postoperative pain, Curr. Pain. Headache Rep. 25 (2021) 3, https://doi.org/10.1007/s11916-020-00920-5.

[64] S. Tarazona, A. Arzalluz-Luque, A. Conesa, Undisclosed, unmet and neglected challenges in multi-omics studies, Nat. Comput. Sci. 1 (2021) 395–402, https://doi.org/10.1038/s43588-021-00086-z.

[65] J. Lötsch, L. Mustonen, H. Harno, E. Kalso, Machine-learning analysis of serum proteomics in neuropathic pain after nerve injury in breast cancer surgery points at chemokine signaling via SIRT2 regulation, IJMS 23 (2022) 3488, https://doi.org/10.3390/ijms23073488.

[66] C. Rönnbäck, E. Hansson, The importance and control of low-grade inflammation due to damage of cellular barrier systems that may lead to systemic inflammation, Front. Neurol. 10 (2019) 533, https://doi.org/10.3389/fneur.2019.00533.

[67] L.J. Hofseth, J.R. Hébert, Diet and acute and chronic, systemic, low-grade inflammation, in: Diet, Inflammation, and Health, Elsevier, 2022, pp. 85–111.

[68] C. Camilli, A.E. Hoeh, G. de Rossi, S.E. Moss, J. Greenwood, LRG1: an emerging player in disease pathogenesis, J. Biomed. Sci. 29 (2022) 6, https://doi.org/10.1186/s12929-022-00790-6.

[69] G.H. Sack, Serum amyloid A - a review, Mol. Med. 24 (2018) 46, https://doi.org/10.1186/s10020-018-0047-0.

[70] R. He, H. Sang, R.D. Ye, Serum amyloid A induces IL-8 secretion through a G protein-coupled receptor, FPRL1/LXA4R, BLOOD 101 (2003) 1572–1581, https://doi.org/10.1182/blood-2002-05-1431.

[71] H.Y. Lee, S.D. Kim, J.W. Shim, H.J. Kim, J. Yun, S.-H. Baek, K. Kim, Y.-S. Bae, A pertussis toxin sensitive G-protein-independent pathway is involved in serum amyloid A-induced formyl peptide receptor 2-mediated CCL2 production, Exp. Mol. Med. 42 (2010) 302–309, https://doi.org/10.3858/emm.2010.42.4.029.

[72] H. Hornero-Ramirez, A. Aubin, M.-C. Michalski, S. Vinoy, C. Caussy, J.-A. Nazare, Multifunctional dietary interventions, low-grade inflammation and cardiometabolic profile: a scoping review, Front. Immun. 15 (2024) 1304686, https://doi.org/10.3389/fimmu.2024.1304686.

[73] D. Furman, J. Campisi, E. Verdin, P. Carrera-Bastos, S. Targ, C. Franceschi, L. Ferrucci, D.W. Gilroy, A. Fasano, G.W. Miller, A.H. Miller, A. Mantovani, C. M. Weyand, N. Barzilai, J.J. Goronzy, T.A. Rando, R.B. Effros, A. Lucia, N. Kleinstreuer, G.M. Slavich, Chronic inflammation in the etiology of disease across the life span, Nat. Med. 25 (2019) 1822–1832, https://doi.org/10.1038/s41591-019-0675-0.

[74] S. Villapol, Roles of Peroxisome Proliferator-Activated Receptor Gamma on Brain and Peripheral Inflammation, Cell. Mol. Neurobiol. 38 (2018) 121–132, https://doi.org/10.1007/s10571-017-0554-5.

[75] M. Hasegawa-Moriyama, T. Ohnou, K. Godai, T. Kurimoto, M. Nakama, Y. Kanmura, Peroxisome proliferator-activated receptor-gamma agonist rosiglitazone attenuates postincisional pain by regulating macrophage polarization, Biochem. Biophys. Res. Commun. 426 (2012) 76–82, https://doi.org/10.1016/j.bbrc.2012.08.039.

[76] D.F.S. Santos, R.R. Donahue, D.E. Laird, M.C.G. Oliveira, B.K. Taylor, The PPARγ agonist pioglitazone produces a female-predominant inhibition of hyperalgesia associated with surgical incision, peripheral nerve injury, and painful diabetic neuropathy, Neuropharmacology 205 (2022) 108907, https://doi.org/10.1016/j.neuropharm.2021.108907.

[77] R.B. Griggs, R.R. Donahue, J. Morgenweck, P.M. Grace, A. Sutton, L.R. Watkins, B. K. Taylor, Pioglitazone rapidly reduces neuropathic pain through astrocyte and nongenomic PPAR-gamma mechanisms, Pain 156 (2015) 469–482, https://doi.org/10.1097/01.j.pain.0000460333.79127.be.

[78] R.B. Griggs, R.R. Donahue, B.G. Adkins, K.L. Anderson, O. Thibault, B.K. Taylor, Pioglitazone inhibits the development of hyperalgesia and sensitization of spinal nociresponsive neurons in type 2 diabetes, J. Pain. 17 (2016) 359–373, https://doi.org/10.1016/j.jpain.2015.11.006.

[79] B.N. Okine, J.C. Gaspar, D.P. Finn, PPARs and pain, Br. J. Pharmacol. 176 (2019) 1421–1442, https://doi.org/10.1111/bph.14339.

[80] P. Jaaks, E.A. Coker, D.J. Vis, O. Edwards, E.F. Carpenter, S.M. Leto, L. Dwane, F. Sassi, H. Lightfoot, S. Barthorpe, D. van der Meer, W. Yang, A. Beck, T. Mironenko, C. Hall, J. Hall, I. Mali, L. Richardson, C. Tolley, J. Morris, F. Thomas, E. Lleshi, N. Aben, C.H. Benes, A. Bertotti, L. Trusolino, L. Wessels, M. J. Garnett, Effective drug combinations in breast, colon and pancreatic cancer cells, Nature 603 (2022) 166–173, https://doi.org/10.1038/s41586-022-04437-2.

[81] R. Odongo, A. Demiroglu-Zergeroglu, T. Çakır, A network-based drug prioritization and combination analysis for the MEK5/ERK5 pathway in breast cancer, BioData Min. 17 (2024) 5, https://doi.org/10.1186/s13040-024-00357-1.

[82] E. Guney, J. Menche, M. Vidal, A.-L. Barábasi, Network-based in silico drug efficacy screening, Nat. Commun. 7 (2016) 10331, https://doi.org/10.1038/ncomms10331.

[83] F. Badrulhisham, E. Pogatzki-Zahn, D. Segelcke, T. Spisak, J. Vollert, Machine learning and artificial intelligence in neuroscience: a primer for researchers, Brain Behav. Immun. 115 (2024) 470–479, https://doi.org/10.1016/j.bbi.2023.11.005.

[84] C. Quesada, A. Kostenko, I. Ho, C. Leone, Z. Nochi, A. Stouffs, M. Wittayer, O. Caspani, N.B. Finnerup, A. Mouraux, G. Pickering, I. Tracey, A. Truini, R. D. Treede, L. Garcia-Larrea, Human surrogate models of central sensitization: a critical review and practical guide, Eur. J. Pain. 25 (2021) 1389–1428, https://doi.org/10.1002/ejp.1768.

[85] L. Arendt-Nielsen, B. Morlion, S. Perrot, A. Dahan, A. Dickenson, H.G. Kress, C. Wells, D. Bouhassira, A.M. Drewes, Assessment and manifestation of central sensitisation across different chronic pain conditions, Eur. J. Pain. 22 (2018) 216–241, https://doi.org/10.1002/ejp.1140.

[86] Eisenach, Preventing chronic pain after surgery: who, how, and when? Reg. Anesth. Pain. Med 31 (2006) 1.